NASA CONTRACTOR
REPORT

Report No. 61286

ANALYSIS OF WIND FIELD CONDITIONS ADVERSELY AFFECTING VEHICLE OPERATIONS

By Joseph L. Goldman

Institute for Storm Research
University of St. Thomas
3812 Montrose Boulevard
Houston, Texas 77006

March 25, 1969

Interim Report

Prepared for

NASA-GEORGE C. MARSHALL SPACE FLIGHT CENTER
Marshall Space Flight Center, Alabama 35812

TECHNICAL REPORT STANDARD TITLE PAGE

1. Report No.	2. Government Accession No.	3. Recipient's Catalog No.
NASA CR-61286		

4. Title and Subtitle	5. Report Date
ANALYSIS OF WIND FIELD CONDITIONS ADVERSELY AFFECTION VEHICLE OPERATIONS	March 25, 1969
	6. Performing Organization Code
7. Author(s)	8. Performing Organization Report No.
Joseph L. Goldman	
9. Performing Organization Name and Address	10. Work Unit No.
Institute for Storm Research University of St. Thomas 3812 Montrose Boulevard, Houston, Texas	11. Contract or Grant No. NAS8-21292
	13. Type of Report and Period Covered Interim March 68 - March 69
12. Sponsoring Agency Name and Address	14. Sponsoring Agency Code
Aero-Astrodynamics Laboratory Marshall Space Flight Center, Alabama 35812	

15. Supplementary Notes

This work was accomplished under the technical monitorship of Mr. John W. Kaufman and Dr. George Fichtl, Aerospace Environment Division, Aero-Astrodynamics Lab, NASA, Marshall Space Flight Center.

16. Abstract

Presented is an analysis of wind field conditions which could adversely affect vehicle operations, with particular application to the prospective launch sites at the Kennedy Space Center. Most turbulence models are based on ground wind data from meteorological towers. This report offers a means of diagnosing and predicting winds from both ground and satellite data. A theoretical model is developed whereby it is possible for the wind profile from the ground upward to be expressed as a function of the immediate past history of the CAOF forced flow. The principal theoretical contribution developed is in the friction layer, and these developments are made in anticipation of real-time forecasting. Also shown is the continuing development of an adverse wind warning system which is based on a theoretical and numerical model of airflow and which has been formulated and programmed for NASA computers.

17. Key Words	18. Distribution Statement
thunderstorm cold air outflow horizontal temperature gradients	FOR PUBLIC RELEASE E. D. GEISSLER Dir, Aero-Astrodynamics Lab, MSFC

19. Security Classif. (of this report)	20. Security Classif. (of this page)	21. No. of Pages	22. Price
Uncl	U	96	

FOREWORD

This report was prepared by the Institute for Storm Research at the University of St. Thomas, Houston, Texas, for the National Aeronautics and Space Administration, Marshall Space Flight Center, Aerospace Environment Divison, Huntsville, Alabama, under Contract NAS8-21292, entitled, "Analysis of Wind Field Conditions Which Adversely Affect Vehicle Operations." Mr. John W. Kaufman and Dr. George H. Fichtl of the Marshall Space Flight Center, Aero-Astrodynamics Laboratory, Aerospace Environment Division, were the technical monitors on behalf of the Contracting Officer, during the administration of the contract, and Mr. William W. Vaughan and Mr. Kelly Hill assisted in the review of the final report. Mr. Joseph L. Goldman was the Princiapl Investigator for the Institute for Storm Research.

TABLE OF CONTENTS

LIST OF ILLUSTRATIONS

GLOSSARY OF SYMBOLS

(In Order of Occurrence)

Symbol	Page	Definition	
ψ	iii	Stream function in numerical outflow model	
z	iii	Height	
z_0	2	Characteristic roughness length (turbulence theory)	
s	13	Minimum averaging time of an instrument	Used only in reference to Brook and Spillane (1964)
t	13	Response time of a device or structure	
CAOF	16	Cold Air Outflow from thunderstorm	
u_*	17	Friction velocity	
τ	17	Shearing stress	
ρ	17	Density	
u', w'	17	Fluctuations of velocity components u and w	
T	18	Averaging time interval (sample length)	
$\overline{u}$	18	Mean velocity	
k	18	Arbitrary constant	
DAIF	32	Dry Air Inflow into thunderstorm	
WAIF	32	Warm Air Inflow into thunderstorm	
φ	33	Velocity potential	
u_r	33	Radial component of wind velocity in polar coordinates	
u_θ	33	Transverse component of wind velocity in polar coordinates	
r, θ	33	Coordinates in polar system	
$\sim$	34	(Tilde) denotes coordinate relative to center of storm	

Symbol	Page	Definition
V_t	34	Translational velocity of the storm
W_c	36	Complex potential for fluid motion

1. SUMMARY

This report is concerned with the analysis of wind field conditions which could adversely affect vehicle operations, with particular application to the prospective launch sites at the Kennedy Space Center. A survey of the literature in this area of research discloses that the information on severe local storms reported by Atlas (1963) is the standard reference. Strong winds have been related to thunderstorm cold air outflow near the ground by Kaufman (1967) and Fichtl (1968). Other references are Fujita (1962) who presented an analysis of maximum outflow winds. Lidga and Bigler (1958) described the profile of wind emanating from a moving source. Brooks (1968) pointed out that convection of warm air may occur on bubbles of warm air, or as a plume of warm air in a continuous updraft. Goldman (1968) postulated a five-layered steady state thunderstorm. Brook and Spillane (1964) developed a forecast method for gusts. Dabbert (1968) investigated the reducing effect of a meteorological tower on measurements of wind speed, and Davis and Newstein (1968) found gust factors decreasing with increasing height. Fichtl (1968) reported on a continuing analysis of wind roughness length depending on wind direction. Darkow (1968) considers his "Energy Index" a good first indicator of severe storm outbreak. An interesting technique for forecasting heavy squalls is presented by Peskov and Snitkovskiy (1968). Browning and Fujita (1965) and Goldman (1968) presented concepts of the generation of

cold outflow air in thunderstorms. Numerical models, without the cold downdraft producing outflow, have been developed by Orville (1967) and Weinstein and Davis (1968).

Most turbulence models which have been developed are based on ground wind data from meteorological towers. This report attempts to offer a means of diagnosing and predicting winds from both ground and satellite data. A theoretical model is developed here whereby it is possible for the wind profile from the ground upward to be expressed as a function of the immediate past history of the CAOF forced flow. The principal theoretical contribution developed is in the friction layer, and these developments are made in anticipation of real-time forecasting.

The cold air outflow emanating from a thunderstorm has been represented in complex potentials by the addition of pure translation flow and pure source flow. Based on that formulation, a numerical model has been developed to represent the outflow affecting a vertical line at any known location with respect to the center of a storm. With vertical velocity and storm motion as inputs the computer program provides the horizontal flow as a function of height. The source of the outflow is programmed to vary its location with height in a spiral about the center of the storm. Parameters defining the radial variation of the vertical velocity were applied for specific cases and computer results obtained. Using an empirically derived distribution of characteristic length, z_0, a log law variation of wind with height is applied to represent the outflow

in the boundary layer. The lower layers of the theoretical model of outflow are being modified with the results of empirical data from specific cases. The resulting model represents cold air outflow that is frictionally retarded by a two-dimensional distribution of horizontal velocity.

The passage of several summertime thunderstorms has been recorded at NASA's 150-meter meteorological tower at Kennedy Space Center, Florida. Temperature and wind data at resolutions of one-half minute down to one-tenth of a second revealed the structure of the leading edge of cold air outflow in a detail never before available.

In addition to verifying previous concepts of cold air outflow, case studies showed that at all levels the wind shifts direction prior to increasing speed, and the time lag between direction and speed changes diminishes with height. During a 5 minute period preceeding the maximum in wind speed, the wind direction can change as much as 60 degrees.

Velocity for time-to-space conversion was obtained from the motion of radar echoes measured at nearby stations. Time-to-space conversion of the tower data indicates a transition length of 7 to 9 km between the undisturbed warm environmental conditions and the cold thunderstorm wind field. The total time for the transition is about 15 minutes.

Initial temperature decrease occurs simultaneously with the first maximum in speed. The temperature drop occurs first and is greatest at the top measurement level, but the isotherms are nearly vertical. At the

maximum in horizontal temperature change, the horizontal temperature gradient is about twice the vertical. Away from this maximum, however, it appears that the reverse is true. The wind shifts and temperature drops seems to reflect the presence of a surface boundary layer about 30 meters deep, since the isolines of wind and temperature sweep back upstream as they near the ground.

Wind distribution in the vertical associated with thunderstorm outflow is studied. Five-second period oscillations were measured at the meteorological tower on 9 May 1967 and recorded on tape at digitized intervals of 0.1 seconds. The phenomena, which lasted for over 20 minutes, had an increasing phase lag in wind direction with height. The level of maximum wind speed, which was 30 meters high during the first part of the period, rose to 60 meters during the final part. These wave-like oscillation measurements are examined here, with the addition of radar pictures and thermal data.

In conclusion, this report shows a continuing development of an adverse wind warning system which is based on a theoretical and numerical model of airflow and has been formulated and programmed for NASA's computers.

This year of research has made an important contribution to the state of the art in a working digital computer program that models three-dimensional thunderstorm outflow, and which can be modified simply by adding subprograms to compute details which will be added from future

theory and measurement. Higher resolution data are expected to enhance the empirical development of the model. Our further efforts should refine and improve on the program as we concentrate on obtaining input parameters for the forecasting model.

2. INTRODUCTION

Adverse wind conditions affecting launch operations from Kennedy Space Center have been described theoretically, studied empirically, and modeled numerically.

Winds that contribute to over-stressing a vehicle at the launch site have been related to thunderstorm cold air outflow near the ground by Kaufman (1967) and Fichtl (1968). Investigations of existing numerical models, e.g., Orville (1967), Weinstein and Davis (1968), have revealed a common deficiency; namely, they fail to take into consideration the cold downdraft which produces outflow.

The state of the art in convection models has not considered a cold downdraft until the recent mathematical development of a model of airflow in a severe storm by Goldman (1968). The downdraft that feeds the cold outflow is parameterized so that inputs from measurements of atmospheric parameters (such as radar echo intensity or wind and temperature from towers in the lower layers), presently used for diagnostic purposes, can be used on a real time basis for prognostication. This model was originally developed to represent the complicated veering and shearing environment of the Great Plains thunderstorm cold air outflow. The less complicated environment of the Florida thunderstorm can be represented by neglecting some of the layers in this model.

The numerical application of this adjusted model consists of a

digital computer program that produces the wind profile at any given location (the launch site in our case) from storm parameters. The time variations of the wind profile are obtained by the time variation of input parameters. The computer program is designed so that known or measureable quantities can be made independent variables and unknowns or predicted parameters can be made dependent variables. The program is written to allow for addition of special prediction subroutines without redesigning the entire program.

A special theoretical refinement was made to represent the turbulent boundary layer in cold outflow. This refinement accounts for the retardation of the wind by the rough condition of the surface. The log-law used for the wind profile near the ground is matched to the existing model flow, and the height of the characteristic velocity, in the log profile, is computed empirically for the area of interest (Fichtl, 1968). We have devised a general analytic form of the characteristic velocity using continuity considerations. The same continuity considerations were used to derive the cold outflow part of Goldman's severe storm model, and we have derived a mathematical function whereby the characteristic velocity can be obtained from immediate past data. A mathematical development similar to this was made by Dyer (1968), but it was not derived from nor applied to thunderstorm cold outflow conditions[1]. The effort presented

[1] Few theoretical developments in microscale meteorology are suitable for application to the convective stability conditions of a thunderstorm environment. We have the task of deciding whether to use existing theoretical

here lends itself to the real-time problem of predicting boundary layer conditions. Tests of conditions appropriate for real-time prediction are discussed in detail.

The present empirical data with which we modify the theoretical model are provided by case studies of thunderstorm outflow, which are made up of data measured at NASA's 150-meter meteorological tower, existing data from the Air Force operated WIND network, and radar echo displays from Daytona Beach. Since only 30 minute averages in WIND network data are available, efforts to modify the modeled flow are restricted by limitations in data resolution. The only two-dimensional modification now possible is along surfaces made up of the storm's motion with respect to the NASA tower[2]. Analyses of meteorological data from the NASA tower on low resolution strip charts and in high resolution digitized form have revealed significant information about changes in the cold air. Preferred periods of changes in wind and temperature are a function of distance and height. The sequence of wind and temperature change is shown to be different than previously assumed. Vertical

---

or empirical functions, or to develop our own functions. We proceed here, via an analytical development, to derive a function. This we expect to modify as more complete case studies of thunderstorm conditions provide necessary empirical data.

[2] Five minute average winds would allow a resolution sufficiently great to make up the lateral dimension, which completes the three-dimensional modification.

and horizontal temperature gradients are nearly equal in magnitude, except at a particular place near the boundary of outflow. Large gradients in temperature are found to coincide with the small gradients in wind, implying the mixing processes that are taking place in the cold air. A periodic change in wind direction with no accompanying change in speed is shown to continue for more than ten minutes during the passage of the boundary of cold outflow. The extent of these fluctuations into the warm air and the sequence of wind change are considered warnings of adverse wind conditions that can be used operationally.

The present method of fixing the empirical data used to modify the theoretical model is to locate the various studies with respect to the radar echo. This is done in the absence of a horizontal distribution of data through points-with-time resolutions comparable to NASA's 150-meter meteorological tower. The placement of each case study about the storm is shown and the particular time-to-space conversion used to obtain the surfaces of empirical data is described in detail.

References

Dyer, A. J., 1968: An evaluation of eddy flux variation in the atmospheric boundary layer. J. Appl. Meteorol., 7, 5, 845-850.

Fichtl, George H., 1968: An analysis of the roughness length associated with the NASA 150-meter meteorological tower. NASA TMX-53690.

Goldman, Joseph L., 1968: The high speed updraft--the key to the severe thunderstorm. J. Atmos. Sci., 25, 2, 222-248.

Kaufman, J. W., and L. F. Keene, 1968: NASA's 150-meter meteorological tower located at the Kennedy Space Center, Florida. NASA TMX-53699.

Orville, Harold D., 1967: Ambient wind effects on the initiation and development of cumulus clouds over mountains--a numerical experiment. Presented at the Nat'l. Amer. Meteorol. Soc. Meeting, New York, January 23-26.

Weinstein, A. I., and L. G. Davis, 1968: A parameterized numerical model of cumulus convection. Report No. 11, Contract GA-777, National Science Foundation, Department of Meteorology, Pennsylvania State University, University Park, 44 pp.

3. LITERATURE SURVEY

Leon F. Graves

Recent literature on severe local storms adds relatively little information to that reported by Atlas (1963). Most of the information on outflow winds is restricted to measurements at the surface in the regular observing network (station spacing of about 100 nautical miles in the United States and less in Europe). Using time-to-space conversion and other techniques that maximize the use of recorded data, Fujita (1962) presented an analysis of maximum outflow winds from a particular storm system (Fig. 1).

The profile of wind emanating from a source moving at 35 mph was described by Ligda and Bigler (1958). This is shown as Fig.2. The large absolute outflow speed, that would be measured at a fixed point such as a tower, is seen to be made up of the speed of the source of outflow (a), and the speed of the outflow (b). The effect of friction on the lower part of the profile, as seen by the depicted return circulations, has been given limited theoretical consideration in the present study, and it is suggested that the investigation be conducted.

Brooks (1963) points out that convection of warm air may occur on bubbles of warm air, or as a plume of warm air in a continuous updraft. When convection leads to a severe storm, the weight of the precipitation starts a downdraft that spreads out as relatively cool air. Goldman

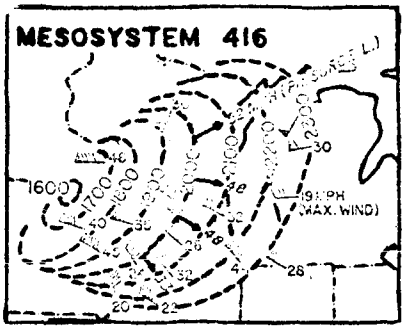

Fig. 1 Maximum wind velocity following the pressure surge line of 5 June 1953.

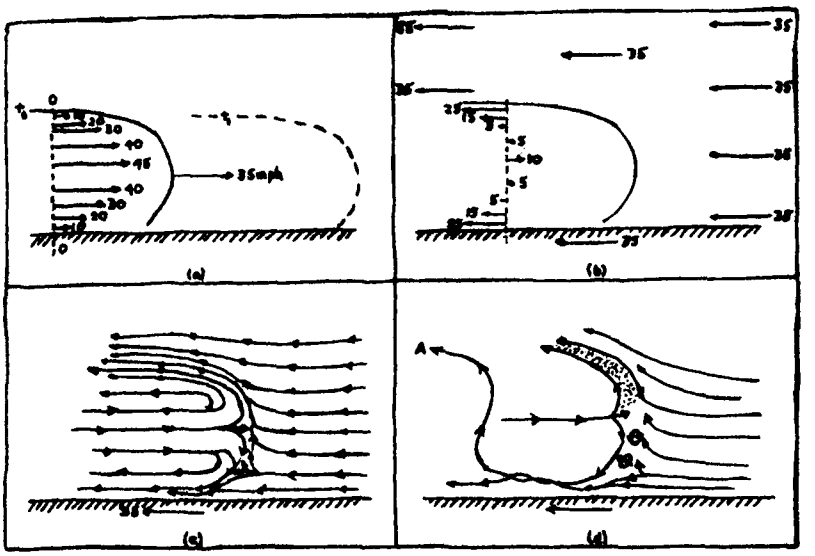

Fig. 2 Circulations associated with an advancing dense air mass. Notice that the overrunning portion of the boundary breaks up into tiny eddies. From Ligda and Bigler (1958).

(1968) postulates a five layered steady state thunderstorm, but does not elaborate on gustiness in the cold air outflow.

The measured data on gustiness of the wind during thunderstorm outflow conditions is highly dependent on instrument response. Brook and Spillane (1964) point out that the minimum averaging time (s) of an instrument measuring wind speed is generally different from the response time (t) of a device or structure affected by the wind. They develop a relationship between the maximum gust averaged over (s) seconds and the maximum gust of (t) seconds duration and present forecasting application.

Dabbert (1968) investigates the effect of a meteorological tower on the measurements of wind speed and finds reductions up to 35% in the wake, with increases up to 19% along the sides, seemingly independent of wind speed. Reasonable corrections can be applied. Using a 1000 foot tower, Davis and Newstein (1968) find that gust factors decrease with increasing height. However their results do not necessarily apply to thunderstorm conditions.

Fichtl (1968) reports that NASA personnel are now developing analytical models of launch vehicles which predict the response of the vehicles to various types of ground forcing functions. His analysis of Kennedy Space Center tower data gives values from 0.23 m to 0.68 m for the wind roughness length depending on the wind direction. This analysis is continuing.

Darkow (1968) examines the total energy environment and considers that his "Energy Index" is a good first indicator of severe storm

outbreak. He points out, however, that the final forecast involves all severe storm parameters.

An interesting technique for forecasting heavy squalls is presented by Peskov and Snitkovskiy (1968). Their method is a variation of the Schowalter stability index where the depth of the layer defined by the condensation level and the height of the -10C isotherm is used instead of the usual pressure levels. They show an inverse relation between that depth and the total wind between the surface and 500 mb. Their described mechanism of mixing dry environmental air with nearly saturated cloud air into which raindrops will fall and evaporate causing negative buoyancy agrees with present concepts of the generation of cold outflow air in thunderstorms, e.g., Browning and Fujita (1965) and Goldman (1968).

References

Atlas, David, et al., 1963: Severe local storms. Meteorol. Monogr., 5, 27, Amer. Meteorol. Soc., Boston, Mass., 247 pp.

Brook, R. R., and K. T. Spillane, 1968: The effect of averaging time and sample duration or estimation and measurement of maximum wind gusts. J. Appl. Meteorol., 7, 4, 567-574.

Brooks, Edward M., 1963: Discussions of Ludlam's paper. Meteorol. Monog., 5, 27, p. 31.

Browning, Keith A., and Tetsuya Fujita, 1965: A family outbreak of severe local storms--a comprehensive study of the storms in Oklahoma on 26 May 1963. AFCRL-65-695(1), 54 pp.

Dabbert, Walter F., 1968: Tower induced errors in wind profile measurements. J. Appl. Meteorol., 7, 3, 359-366.

Darkow, Grant L., 1968: The total energy environment of severe storms. J. Appl. Meteorol., 7, 2, 199-205.

Davis, Francis K., and Herman Newstein, 1968: The variation of gust factors with mean wind speed and with height. J. Appl. Meteorol., 7, 3, 322-328.

Fichtl, George H., 1968: Characteristics of turbulence observed at the NASA 150-m meteorological tower. J. Appl. Meteorol., 7, 5, 838-844.

Fujita, Tetsuya, 1962: A review of researches on analytical mesometeorology. Mesometeorology Project Research Paper No. 8, Department of Geophysical Sciences, University of Chicago, 114 pp.

Goldman, Joseph L., 1968: The high speed updraft--the key to the severe thunderstorm. J. Atmos. Sci., 25, 2, 222-248.

Ligda, M.G.H., and S. G. Bigler, 1958: Radar echoes from a cloudless cold front. J. Meteorol., 15, 494-501.

Peskov, B. Ye, and A. I. Snitkovskiy, 1968: Forecasting heavy squalls. Meteorologiya i gidrologiya, 9, 52-57.

4. THEORETICAL MODEL OF OUTFLOW

Michael D. Reifel and Joseph L. Goldman

A model used to represent the adverse winds that could result from thunderstorms was developed previously by this group (Goldman 1968) for use in studying the Great Plains severe storms. Its generality, however, allows us to adjust its many mathematical complexities to fit the particular environment of interest. In applying the model to storms in Florida, the environment is simplified and we can neglect some of the layers.

In the following paper on the numerical model the flow is shown in its mathematical form for the cold air outflow (CAOF) layer that extends to about 1500 feet above the ground. The complete mathematical formulation of the model as given by Goldman (1968) can be followed in greater detail in the reports of Goldman and Freeman (1966) and Goldman (1967).

The principal theoretical contribution developed here was in the friction layer, the lowest levels of flow in the CAOF. A method is developed whereby it is possible that the wind profile from the ground upward can be expressed as a function of the immediate past history of the forced flow (CAOF). This development is made in anticipation of the real-time forecast problem, when speed as well as accuracy will be important.

In general, turbulence models have been developed which are based on ground wind data from meteorological towers. In the absence of vertical velocity fluctuation data a profile law is used to calculate

turbulent shear stress, and as a velocity scaling parameter to combine turbulence data in the form of spectra, cospectra, variances, etc., based on similarity considerations.

In this paper vertical velocity fluctuation data is determined from existing longitudinal velocity fluctuation data through continuity considerations. Then the surface friction velocity is calculated directly, and von Kármán's similarity constant is determined for a sudden thunderstorm through a wind profile law.

A. Theoretical Approach

In comparison with aerodynamic boundary layers, meteorological surface layers are usually thick, and the region that is of primary interest (and accessible for measurement) is relatively small and close to the surface. The actual thickness and possible growth of these layers are often assumed to be of little importance, so it is customary to treat them theoretically as if the properties near the surface were independent of the state of the flow at great heights. Consequently the turbulent shear stress and heat flux are often considered to be independent of height.

Since the change of the turbulent stress vector is assumed negligible in the surface layer, "a friction velocity", constant with height, can be defined by

$$u_* \equiv \sqrt{\tau/\rho} = \sqrt{-\overline{u'w'}} \qquad (1)$$

where τ is the shear stress, ρ is the atmospheric density near the surface, and u', w' are the parallel and vertical components of the velocity fluctuations about the mean wind, $\bar{u}$. The overbar below denotes the time averaging operator

$$\overline{(\quad)} \equiv \frac{1}{T} \int_{t_1}^{T+t_1} (\quad)\, dt ,$$

where T is the interval of time over which the averaging process is performed.

If the surface layer is assumed incompressible with steady mean flow only in the x direction, the mean wind profile in the first 30 to 60 meters of the atmosphere, in conditions of neutral stability (when there is no heat flux), is obtained by the Monin-Obukhov similarity hypothesis (Lumley and Panofsky, 1964) by

$$\bar{u} = \frac{u_*}{k} \ln (z/z_0) \qquad (2)$$

where $\bar{u}$ is the mean wind velocity at height z, z_0 is the length characterizing the roughness of the surface (below z_0, the mean flow vanishes because the flow below z_0 has been disrupted to the extent that the flow is completely turbulent), u_* is the friction velocity defined above, and k is the von Kármán constant.

The constant k, which is primarily an intuitive concept, is added for convenience in similarity. Current knowledge of this term has been derived from a hierarchy of empirical investigations and has a numerical

value of about 0.4 (Rider, 1954). (We will find that this is not always the case.)

If the velocity components are decomposed into time-averaged and fluctuation terms, and substituted into the continuity equation for incompressible two-dimensional flow, and the resulting equation time-averaged term-by-term, the continuity equation for our two-dimensional model becomes

$$\frac{\partial \bar{w}}{\partial z} = -\frac{\partial \bar{u}}{\partial x}$$

$$\frac{\partial w'}{\partial z} = -\frac{\partial u'}{\partial x} + \frac{\partial v'}{\partial y} \qquad (3)$$

where the bar indicates time-averaged (or mean) quantities and the prime indicates fluctuation quantities.

The G.I. Taylor hypothesis (Lumley and Panofsky, 1964) implies that for certain conditions (including v' uncorrelated with u') the continuity equation for the fluctuation terms can be written

$$\frac{\partial w'}{\partial z} = \frac{1}{\bar{u}} \frac{\partial u'}{\partial t} \quad . \qquad (4)$$

Using Eq. 4 the vertical fluctuation velocity is obtained from longitudinal fluctuating velocity information by

$$w'(z,t) = w'(z_1,t) + \int_{z_1}^{z} \left(\frac{1}{\bar{u}} \frac{\partial u'}{\partial t} \right) dz \qquad (5)$$

Then the surface friction velocity is obtained from Eq. 1 after applying

the averaging operator for a sufficient interval of time.

B. Experimental Data

Ground wind data were obtained from measurements made by NASA on their 150-meter meteorological tower at Kennedy Space Center, Florida. The tower is instrumented at the 3, 18, 30, 60, 90, 120 and 150 meter levels with Climet wind sensors (Model CI-14) and, in addition, is instrumented at the 18, 60, 120 and 150 meter levels with Climet aspirated thermocouples (Model 016) (Kaufman and Keene, 1968).

The measurements, recorded every 1/10 second on high resolution magnetic tape, for tests of duration ranging between one-half to one hour, are from cases obtained during the hours between 1300 and 2000 EST. Specifically, our conclusions are based on data for two typical sudden thunderstorms; the tests for wind speed and direction, made at the 3, 18 and 30 meter levels for 10 minutes duration, occurred at 1600 and 1900 EST.

Fichtl (1968) determined the surface roughness length, z_0, for the 150-meter tower location from thirty-nine wind and temperature profiles evaluated at the 18 and 30 meter levels. For those wind directions θ, in the ranges $0^0 \leq \theta < 150^0$, $180^0 \leq \theta < 240^0$ and $300^0 \leq \theta < 360^0$, the roughness length is 0.23 m; for those wind directions in the ranges $150^0 \leq \theta < 180^0$ and $240^0 \leq \theta < 300^0$, the roughness length has the values 0.51 m and 0.65 m, respectively.

C. Numerical Analysis

To evaluate the integral of Eq. 5 it is expedient to adopt a simple linear interpolation between adjacent heights in both the vertical and time dimensions. Eq. 5 then becomes

$$w'(z,t) = w'(z_1,t) + \left(\frac{\Delta z}{4\Delta t}\right)\left\{\left[\frac{u'(t+\Delta t) - u'(t-\Delta t)}{\bar{u}}\right]_z + \left[\frac{u'(t+\Delta t) - u'(t-\Delta t)}{\bar{u}}\right]_{z_i}\right\} \quad (6)$$

where $w'(z,t)$ is the vertical fluctuating wind velocity measured at z height, z_i is the adjacent height, Δz is the height increment, $u'(t)$ is the longitudinal fluctuating wind velocity measured at height z (or z_i) for instant t, Δt is the time increment between measurements, and $\bar{u}$ is the steady wind velocity at height z (or z_i).

Since at ground level the steady and fluctuating wind velocity components are zero (i.e., at $z = 0$, $u = u' = w' = 0$) (6) can be generalized to

$$w'(z,t) = \left(\frac{1}{4\Delta t}\right)\sum_{i=1}\left(\Delta z_i + \Delta z_{i+1}\right)\left[\frac{u'(t+\Delta t) - u'(t-\Delta t)}{\bar{u}}\right]_i \quad (7)$$

D. Results

Time and length scales of turbulent motion that serve to transport properties are quite large, often of the same order as time and length of

scales characterizing the distribution of properties being transported. Hence, before Eq. 6 can be solved successfully, appropriate time and length scales must be determined.

As previously noted, tower measurements are recorded every 1/10 second on high resolution magnetic tape. To determine a sufficient interval of time over which the averaging process must be performed while calculating the mean distribution of properties, the mean wind speed, $\bar{u}$, was calculated for various time periods. Mean wind speed was calculated for T of 60, 120 and 300 seconds duration using measurement data from the 18 meter level that was averaged for each one second increment. Mean wind speed was then calculated for T of 300 seconds duration using measurement data from the 18 meter level that were averaged for each 10 second increment, and then for each 30 second increment. Finally, mean wind speed was calculated for T of 600 seconds duration using measurement data averaged for each 10 second increment. The results of these calculations are given in Fig. 3.

Since data were available from only one tower location, spacial information could be obtained in only one dimension. Under certain conditions, the Taylor hypothesis allows the use of data from only one location to be used for spacial analyses by doing the analyses in the time domain. Basically, if the mean wind speed is high enough, the turbulence will not have time to change as it is being convected past the tower.

Panofsky, et al., (1958) found that Taylor's hypothesis is valid close

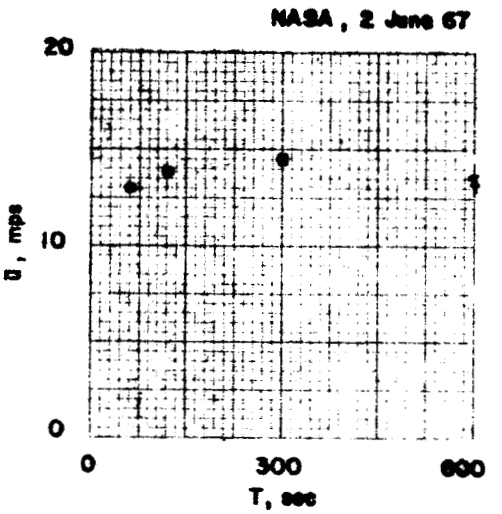

Fig. 1. Mean wind speed at 18 meters for various time periods.

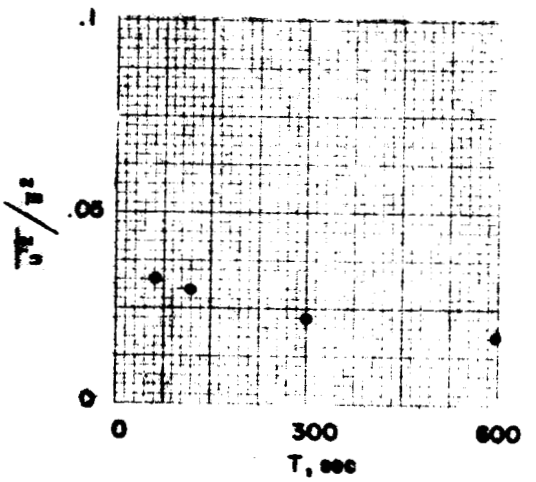

Fig. 2. Taylor Hypothesis criteria.

to the ground for lag distances up to 90 meters and levels of $\overline{(u')^2}/\bar{u}^2 \sim 1/9$ and smaller. These Taylor hypothesis criteria are shown in Fig. 4 for the various time periods.

The recorded data is averaged to eliminate the higher orders of fluctuations because the Taylor hypothesis is only a first approximation for the velocity as a whole. Fig. 3 indicates that the increment over which the data is averaged, or the time period used for determining the mean wind speed, has no significant effect on the acutal mean wind speed. This, however, is not true for the conditions necessary to satisfy Taylor's hypothesis, as seen in Fig. 4. In fact, a dilemma arises from the criteria.

For mean wind speed as indicated, data averaged at increments of 10 or 30 seconds would not satisfy the 90 meter lag distance criterion. However, it was later discovered that the approximate method for evaluating the integral in Eq. 5 was sensitive to the increment of data used. The dilemma was circumvented by using data averaged at 10 second increments to evaluate the integral at 1 second increments.

After programming Eq. 7, Eqs. 1 and 2 were programmed for solution by a digital computer (see computer program FORTRAN listing at the end of this paper), and the mean wind velocity profiles were determined for two tests of 600 seconds in duration, occurring at 1603 hours on 2 June 1967 and 1927 hours on 11 June 1968. The mean wind velocity profiles are shown in Fig. 5.

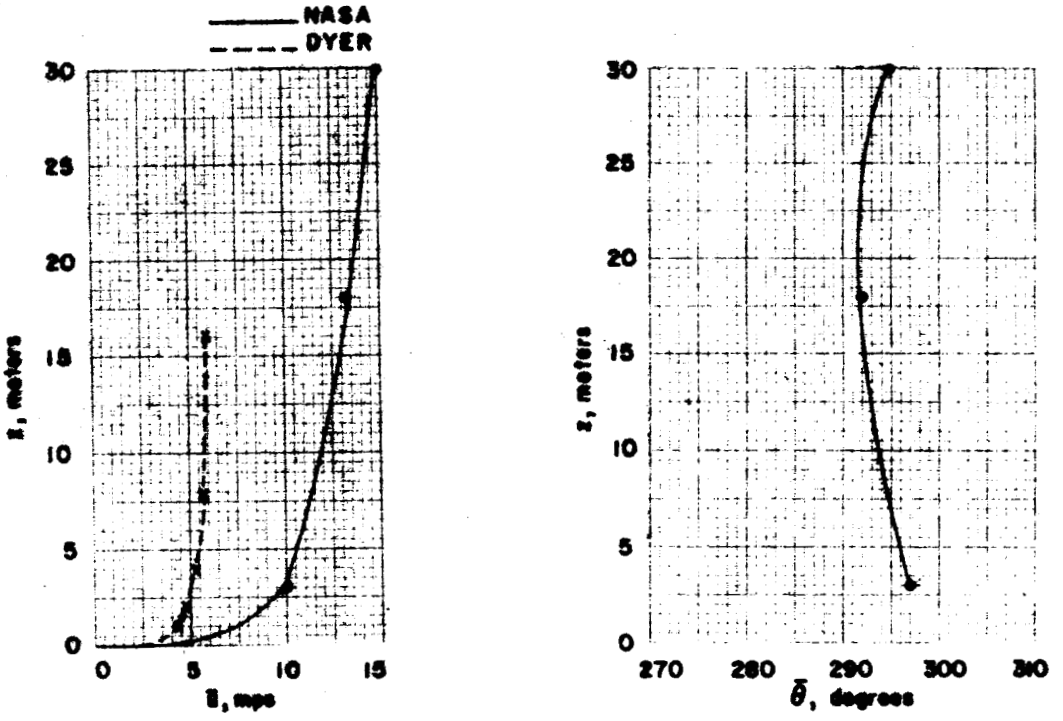

Fig. 5. Mean wind speed and direction profiles.

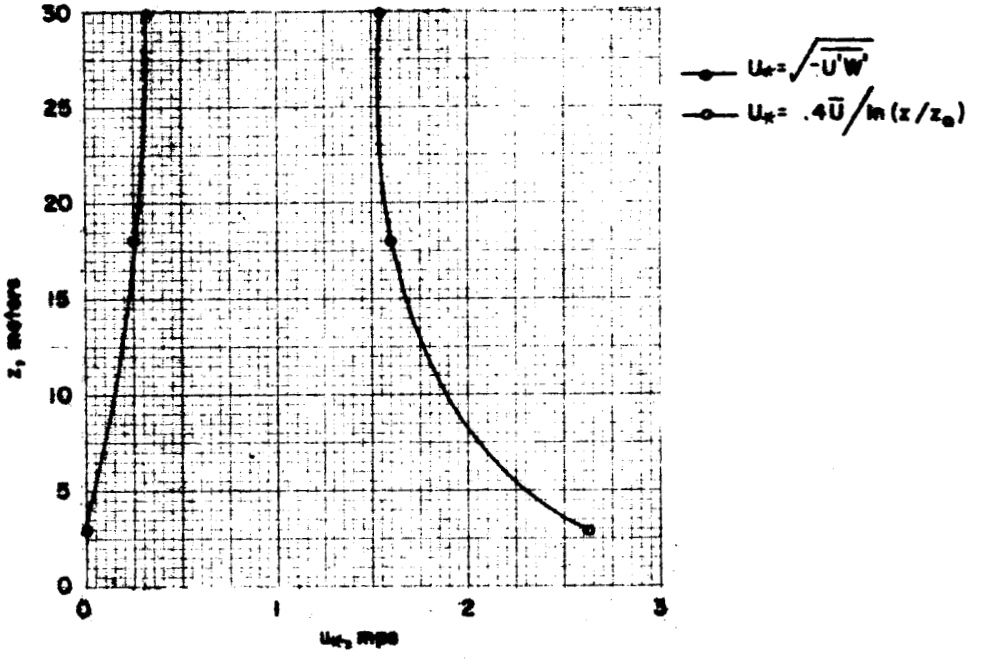

Fig. 6. Friction velocity from Equation 1 and Equation 2.

The mean wind velocity profiles are used to determine the profile of the longitudinal velocity fluctuations for any time interval. Then the vertical velocity fluctuations are found from Eq. 7. The friction velocity, calculated from both Eqs. 1 and 2, is shown in Fig. 6. The curves calculated from the two equations diverge as $z \to 0$ because $\ln(z/z_0) \to 0$, as $z \to z_0$, and $\overline{u'w'} \to 0$, as $z \to 0$.

The von Kármán constant, k, can be determined for the boundary layer by elimination between Eqs. 1 and 2. This constant is shown in Fig. 7.

E. Conclusions

Fig. 5 confirms the Monin-Obukhov similarity hypothesis, i.e., $\bar{u} \sim \ln(z/z_0)$; but Fig. 6 strongly indicates the basic assumption that friction velocity is constant with height, and is not valid in the lower regions of the boundary layer. Moreover, Fig. 7 shows that the von Kármán constant is not a constant at all in these lower regions, but instead is a function of height. As height increases and wind conditions approach those of the free stream, both the friction velocity and the von Kármán constant tend to become independent of height, but the constant k obtains a value much different from the conventional 0.4 value (Fig 7 shows that for our wind data, k approaches a value between 0.08 and 0.1).

We can assume then that either the local stress in terms of the mean distributions is not in general described by local conditions (i.e., Eqs. 1 and 4 are invalid), or the basic assumptions regarding our boundary

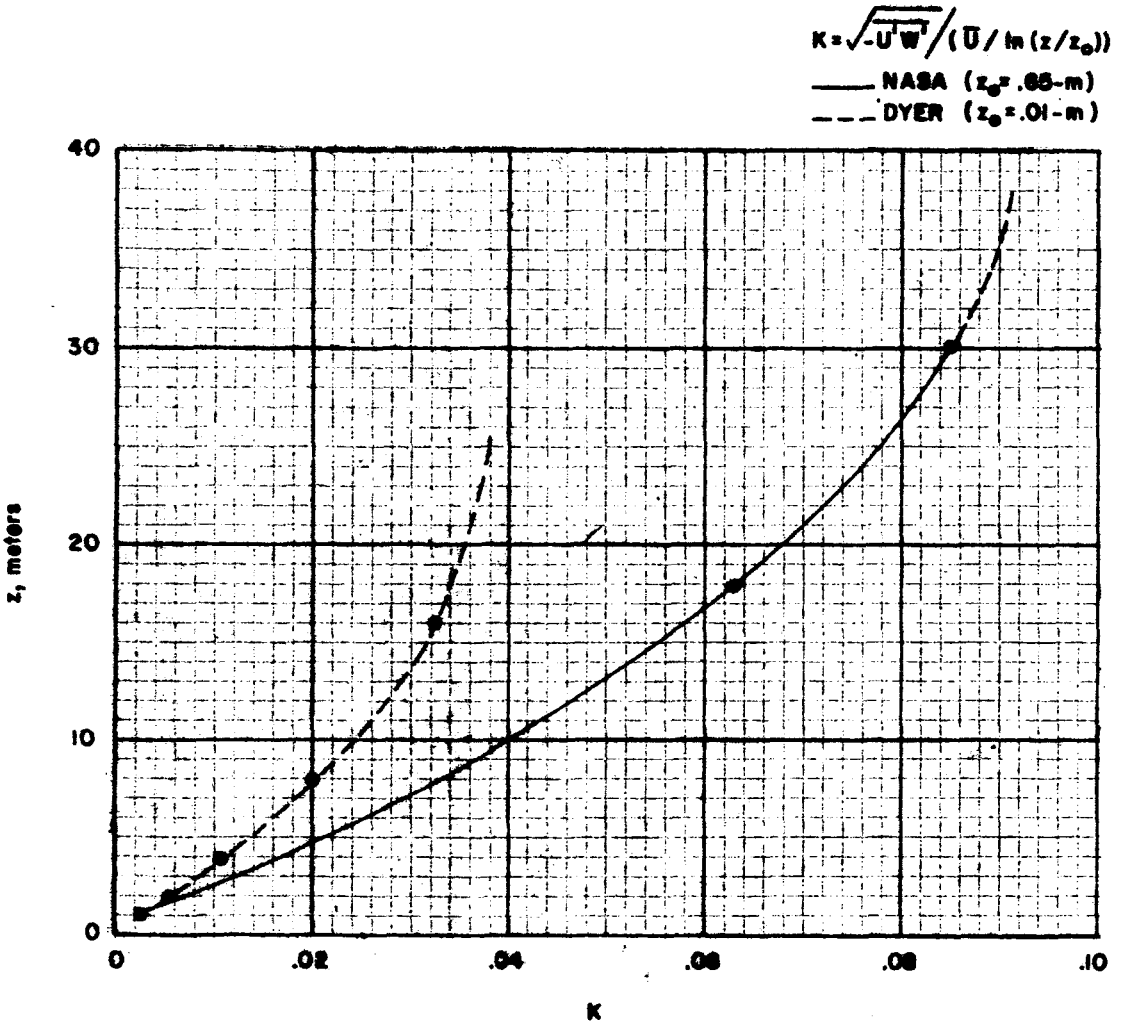

Fig. 7. von Kármán constant in boundary layer.

layer simulation must be revised. In order to eliminate the question of validity of Eq. 4, data from a paper by Dyer (1968) was used to make independent calculations of the friction velocity and von Kármán constant. This data, measured at two tower locations separated by 200 meters, represents an average of measurements for each 30 minute duration (which puts a strain on the validity of Eq. 3). The results of these calculations are shown in Fig. 7.

The results of the calculations from the Dyer data somewhat confirm the results obtained from the NASA data. Hence, we can only conclude that the basic assumptions underlying the classical meteorological boundary layer simulation must be re-examined.

F. Suggestions For Future Work

Due to the above findings it is suggested that the basic assumptions underlying meteorological boundary layer simulation be closely re-examined. The following suggestions should be considered:

1. A larger quantity of available NASA data should be analyzed;
2. Since the von Kármán constant, as an intuitive concept, is predicated also upon the simulation of heat flux, the assumption of neutral stability should be reconsidered and the heat flux situation examined;
3. The assumption regarding the definition of a friction

velocity should be examined:

4. An experiment should be devised whereby the vertical wind velocity can be measured;
5. Finally, a model of the boundary layer reflecting the fact that turbulence is a three-dimensional phenomenon should be developed.

In the opinion of one of the authors (Goldman) an alternative approach to defining u_* in terms of immediate past history is to use the average system velocity, $\vec{c}$, to convert the time variable tower data to space variable data.

Previously we used the G. I. Taylor hypothesis, which is best for turbulence conditions where processes are entirely stochastic. However, we have here some determinism, namely, the radar measured motion of the system causing the outflow. Therefore we can test, using that velocity, to see if we can compute the profile.

As was done before, we define

$$u_* = \sqrt{\overline{u'w'}} \tag{8}$$

From the equation of continuity

$$w'(z) = w'(z_0) - \left(\frac{\partial u'}{\partial r} + \frac{u'}{r}\right) \int_{z_0}^{z} dz \tag{9}$$

where u' is the perturbed radial component of the velocity in the polar

co-ordinates system of the numerical model, r is the radius, and w' is as defined above. Since the average indicated by the overbar in Eq. 8 is taken over the entire layer and the surface z_0 is where $u' = 0$, then

$$\left(\frac{\partial u'}{\partial r} + \frac{u'}{r}\right) = \frac{1}{2}\left[\frac{\partial u'(z)}{\partial r} + \frac{u'(z)}{r}\right] \tag{10}$$

Now, we assume

$$\frac{\partial u'}{\partial r} = \frac{1}{|\vec{c}|}\frac{\partial u'}{\partial t} \tag{11}$$

where u' is measured at the tower. The averaging interval is determined by the time period over which the calculated echo velocity $\vec{c}$ is valid.

Using 10 minute averages with systems moving at 15 m sec^{-1} results in defined perturbations less than 9 km in length. This is the length, found in one case study, which extends through the mixing zone from the warm to cold air.

7. References

Dyer, A. J., 1968: An evaluation of eddy flux variation in the atmospheric boundary layer. J. Appl. Meteorol., 7, 845-850.

Fichtl, George H., 1968: An analysis of the roughness length associated with the NASA 150-meter meteorological tower. NASA TMX-53690.

Goldman, Joseph L., 1968: The high speed updraft--key to the severe thunderstorm. J. Atmos. Sci:, 25, 2, 222-248.

_____, 1967: A parameterized model of air circulation and rain distribution in severe storms. Final Report, NSSL, Contract No. E-36-67(N), Institute for Storm Research, Inc., Houston, Texas, 76 pp.

Goldman, Joseph L., and John C. Freeman, 1966: The development of a model of air circulation and rain distribution in a steady state severe storm. Final Report, NSSL, Contract No. Cwb-11367, Institute for Storm Research, Inc., Houston, Texas, 55 pp.

Kaufman, J. W., and L. F. Keene, 1968: NASA's 150-meter meteorological tower located at the Kennedy Space Center, Florida. NASA TMX-53699.

Lumley, J. T., and H. A. Panofsky, 1964: The Structure of Atmospheric Turbulence. New York, Interscience Publishers, John Wiley and Sons, Inc.

Panofsky, H. A., et. al., 1958: The relation between Eulerian time and space spectra. Quart. J. Roy. Meteorol. Soc., 84, 270.

Rider, N. E., 1954: Eddy diffusion of momentum, water vapor and heat near the ground. Phil. Trans. Roy. Soc., A246, 481.

5. NUMERICAL MODEL OF OUTFLOW

Joseph L. Goldman, Sam B. Rosenberg and Frances Miller

When applying Goldman's (1968) model of airflow to the cold outflow layer of the thunderstorm, the curving displacement of the downdraft with height and its change in shape become important. As was explained in the derivation of cold air outflow (CAOF) layer (Goldman and Freeman, 1966; Goldman, 1967 and 1968) the cold air originates on the wake side of the storm in the dry air inflow (DAIF) layer, which is located in middle levels above the warm air inflow (WAIF) layer. Cold air is produced when the DAIF air mixes with nearly saturated cloud air, on the wake side of the storm, while rain falls through the mixed air. Some of the rain evaporates, which cools the mixed air and makes it negatively buoyant. This rain cooled air accelerates downward from its origin near the cloud edge and falls through upward accelerating WAIF air that is converging toward the storm center. The two effects on the cold downdraft caused by flow interaction are a spiral path and a constriction of the tube of cold air as it is drawn toward the center of the storm.

Limits on the orientation of the spiral with respect to the storm center are determined by the orientation of the WAIF which is a function of storm motion and ambient warm moist air flow. The degree of the spiral and the amount of constriction are a function of convergence of the WAIF within the radius of cloud boundary. Computer inputs to control these effects

are implicit in the motion and intensity of the radar echo of the storm when combined with reliable ambient wind information for the WAIF layer. Although the state of the art does not contain specific numbers, estimates consistent with other knowns of the problem can be made that will be corrected empirically.

A. Computer Program

A master program sequences among the various subprograms, each of which performs a major phase of the calculations: viz, computation of the spiral equation which represents the location and shape of the source of cold air and the CAOF as a function of altitude z ; calculation of the velocity potential φ and the stream function ψ in any specified region of space; and computation of u_r and u_{θ_r}, the radial and transverse components of wind velocity in the same region of space.

In order to effect a precise correlation among the various computations an underlying polar co-ordinate system (r,θ) has been developed. The origin may be arbitrarily designated, but for actual computations the launch site has been used. The polar axis is horizontal to the right and θ is measured counterclockwise.

B. The Spiral Equation for the CAOF

The equation representing the CAOF spiral has been developed in terms of co-ordinates relative to the center of the storm. Consider the projection of the spiral on the $z = 0$ plane (see Fig. 1), where:

V_t — is the storm's translational velocity.

$(\tilde{r}_1, \tilde{\theta}_1)$ — is the position of the CAOF at altitude z_1, relative to the center of the storm C.

$(\tilde{r}_0, \tilde{\theta}_0)$ — is the position of the CAOF at altitude $z_0 < z_1$, relative to the center of the storm.

$(\tilde{r}_w, \tilde{\theta}_w)$ — is the position of the CAOF at altitude $z = 0$, where θ_w is the direction of the Warm Air In Flow (WAIF).

The spiral equation:

$$\tilde{r} = \frac{a(\tilde{\theta} - \tilde{\theta}_w)}{\theta - b} + r_w \qquad (1)$$

with $\tilde{r}$ and $\tilde{\theta}$ relative to the center of the storm, was forced to pass through the three above known points (see Fig. 8) by solving for the parameters a and b.

A linear fractional transformation was developed to express $\tilde{\theta}$ as a function of z. Thus, given a particular altitude, the location of the CAOF at the altitude z can be calculated relative to the center of the storm.

Given:

θ_s — the angle from the polar axis at the launch site to the center of the storm,

θ_{v_t} — the angle which V_t makes with a polar axis passing through the center of the storm and parallel to the one at the launch site,

r_s — the distance from the launch to the center of the storm,

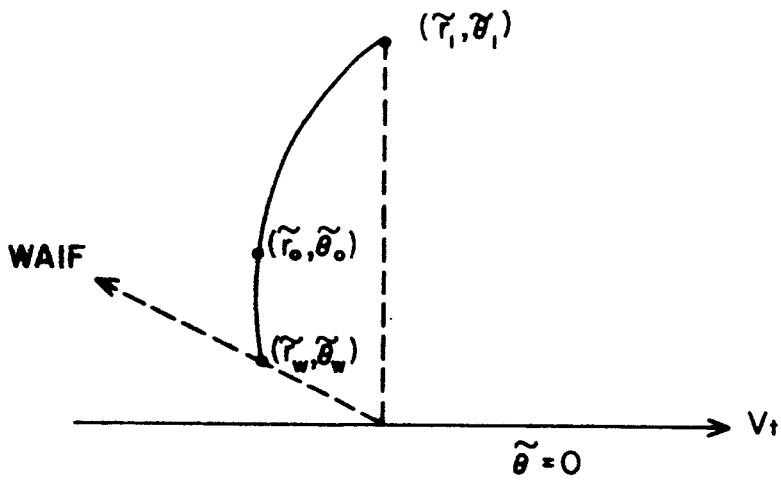

Fig. 8. Graph of a spiral for CAOF.

a transformation of co-ordinates was devised to express the location of the CAOF as $\left[r_c(z) , \theta_c , (z) \right]$, relative to the launch site.

C. The Velocity Potential φ and the Stream Function ψ

The complex potential of the motion of the fluid is defined as:

$$W_c = \varphi + i\psi \tag{2}$$

For a source of strength m at the point $Z_0(z)$ and a uniform stream with velocity V_t, addition of the corresponding complex potentials gives:

$$W_c = - m \ln \left[Z - Z_0(z) \right] - V_t Z \tag{3}$$

where $Z = x + iy$.[1]

Transforming to polar coordinates with origin at the launch site and equating the real and imaginary parts of W_c to φ and ψ, respectively, yields:

$$\varphi(r, \theta_r, z) = - m \ln \left| \left\{ r^2 + r_c^2(z) - 2r\, r_c(z) \cos \left[\theta_c(z) - \theta_r \right] \right\}^{1/2} \right| - V_t \rho \cos\theta \tag{4}$$

$$\psi(r, \theta_r, z) = - m\gamma - V_t \rho \sin\theta \tag{5}$$

where:

[1] A complete derivation of potential flow using the above notation is given by Milne-Thomson (1950).

$$\rho = \left[r^2 + r_s^2 - 2 r r_s \cos(\theta_s - \theta_r) \right]^{1/2} \tag{6}$$

$$\theta = \theta_s - \pi - \theta_{v_t} + \arccos\left[(\rho^2 + r_s^2 - r^2)/2\rho r_s \right] \tag{7}$$

$$\gamma = \arctan\left(\frac{\rho \sin\theta - \tilde{r} \sin\tilde{\theta}}{\rho \cos\theta - \tilde{r} \cos\tilde{\theta}} \right) \qquad -\pi \leq \gamma \leq \pi \ . \tag{8}$$

The source strength m is expressed as a function of z. The vertical wind velocity w by

$$w = -w_m(z_m) \frac{\left(z - z_m\right)^2}{z_m^2} \ e^{-r^2/2\sigma^2(z)} \tag{9}$$

where $w_m(z_m)$ is the maximum vertical velocity occurring at the fixed altitude z_m, and $\sigma(z)$ is the standard deviation of the normal distribution specifying the distribution of w at altitude z. Note: $\sigma(z)$ is assumed to be linear: $\sigma(z) = Qz + s$. The continuity equation:

$$\frac{\partial\left(rV_r\right)}{\partial r} = \frac{-\partial(rw)}{\partial z} \tag{10}$$

is then integrated with respect to r from 0 to R_1, where R_1 is the radius at which all flow becomes horizontal[2].

Since $m = R_1 V_r(R_1)$, this yields:

[2]A complete derivation of the mathematical formulation can be found in Goldman (1968). Specific details and physical interpretation is given in Goldman and Freeman (1966) and Goldman (1967).

$$m = w_m(z_m)\frac{(z - z_m)}{z_m^2}\left\{2\sigma^2(z)\left[1 - e^{\frac{-R_1^2}{2\sigma^2(z)}}\right]\right.$$

$$\left. + 2(z - z_m)Q\sigma(z)\left[1 - e^{\frac{-R_1^2}{2\sigma^2(z)}}\left(\frac{R_1^2}{2\sigma^2(z)} + 1\right)\right]\right\} \qquad (11)$$

D. Results

Plots of ψ have been produced at various altitudes z, ranging from $z = 30$ to $z = 1500$ meters at different values of the source strength, m. These plots extend from 100 meters to 120 kilometers in distance from the launch site. In addition, both θ_{v_t}, the direction in which the storm is moving, and V_t, the storm velocity, have been varied to simulate the effects of storms approaching or leaving both the area and the launch site.

Values of φ and ψ are being produced over a specified region for subsequent manual plotting and contouring. This region is designated through the input parameters:

z — altitude,

R_i — initial radius,

R_f — final radius,

ΔR — radial increment,

θ_i — initial angle,

θ_f — final angle, and

$\Delta\theta$ — angular increment for the computation.

All radii and angles are measured from the origin at the launch site.

Thus it is possible to obtain both horizontal (z = constant) and vertical (r = constant) profiles of φ and ψ. For an illustrative example of a computed horizontal profile of ψ see Fig. 9.

A three-dimensional plexiglass model of the streamlines has been constructed. The projected goal of this computer program is to produce plots printed in the form of maps.

E. Future Work

When the radial and transverse components of wind velocity due to the source m are given by the formulas:

$$u_r = -\frac{1}{r}\frac{\partial x}{\partial \theta_r} = -\frac{\partial \theta}{\partial r} \tag{12}$$

$$u_r = \frac{\partial x}{\partial r} = -\frac{1}{r}\frac{\partial \theta}{\partial \theta_r} \tag{13}$$

then from given formulas (4) and (5) for $\theta(r,\theta_r,z)$ and $x(r,\theta_r,z)$, one may derive analytic formulas for u_r and u_{θ_r} in terms of already known quantities. Then u_r and u_{θ_r} can be plotted over the same region as are θ and x. The components u_r, u_{θ_r} are to be mapped along a chosen radial from the launch site. These are found by transforming the stream function, x, from an origin at the storm center, to an origin at the launch site.

The layer from the ground (z = 0) to $z_0 = 30$ m has purposely been left out of the present program while we are awaiting results of the theoretical

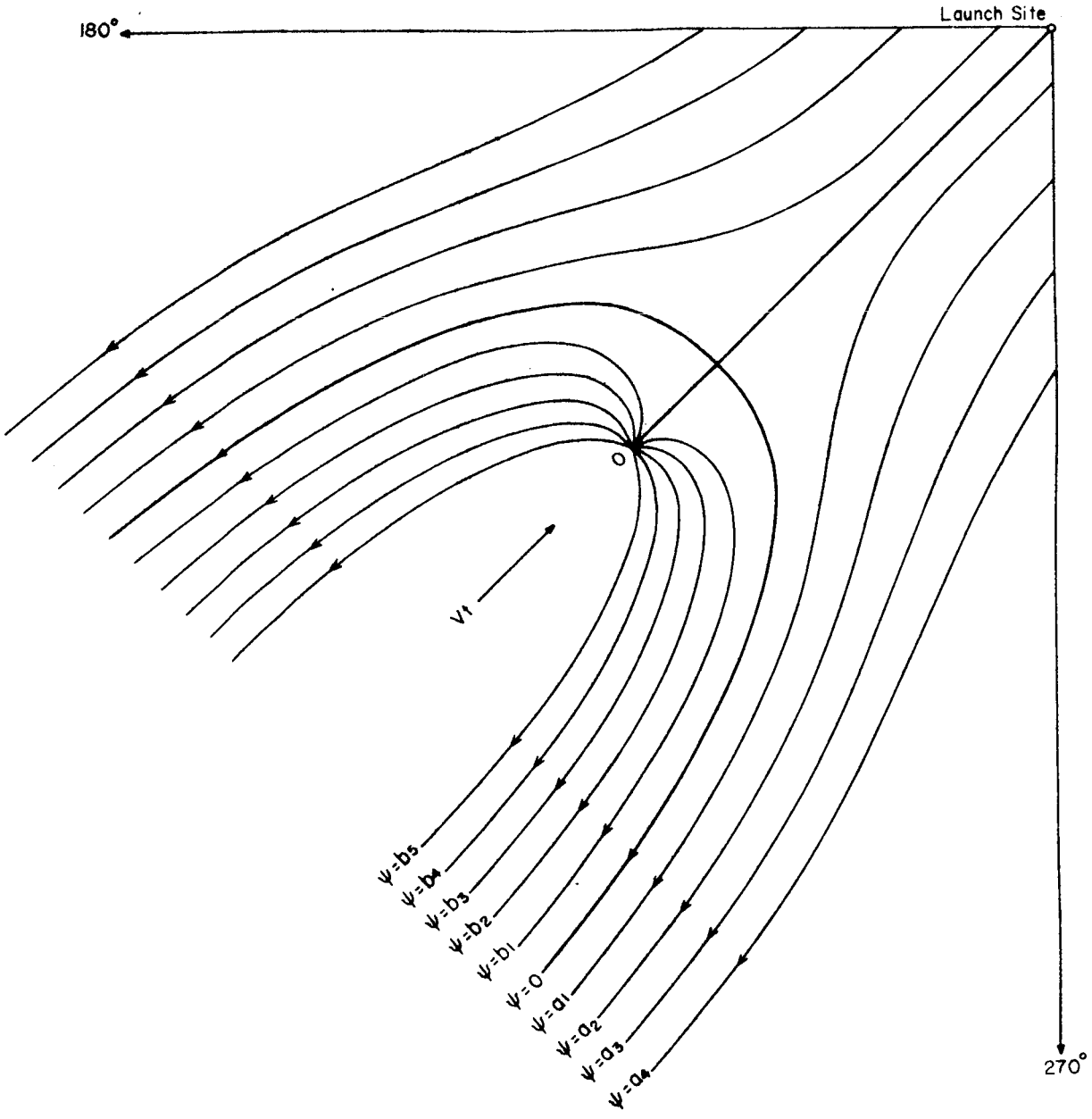

Fig. 9 Plot of stream function ψ for constant value of z, where Vt is the translation velocity of the storm.

study that will permit the use of immediate past history to determine the friction effected velocity. The equations for the layer $0 \leq z \leq 30$ m will be combined into another subprogram, which will allow us the freedom of using either it or substituting other programs that may be developed.

The inclusion of the boundary layer in the final program will be in the form of matching equations for the log profile and outflow profile that will be solved for the height and magnitude of the maximum velocity. While this is a sophisticated process to get the desired output, it is believed that it will best serve when we are faced with the real-time forecasting problem.

F. Forecasting with the Model

For forecasting the wind profile of a storm moving in the vicinity of the launch site, the desired computer output will be a wind profile at the site that changes with time. This desire was anticipated since the u_r and u_{θ_r} components can be chosen for comparison of a radial from the launch site that parallels the motion of the storm. The change in the storm's motion with time will be represented by a change in radial with time, so that the final computer output will be a wind profile with forecasted changes to occur at the site.

The geometric problem having been solved, this leaves the ever present problem of forecasting the storm motion, V_t, that has purposely been kept an input parameter because of inherent difficulties: a "state

of the art" does not exist for forecasting individual thunderstorm motion on a routine basis. Extensive research and study has shifted to the more sensational and anomalous motions that have been observed with severe storms of the Great Plains. The thunderstorms of Florida have been examined recently particularly for atmospheric variables such as hail (Gerrish and Hiser, 1965). Data on their motion however, stems from the early work of the Thunderstorm Project (Byers and Braham, 1949). If attention is given to their conclusions regarding the motion of storms ignoring the explanation of momentum exchange given for the motion, it can be concluded that storms are influenced by the environmental winds in which they are imbedded. The manner by which the environmental winds affect motion is a subject of intensive theoretical consideration based on recent observations and measurements of the Great Plains Severe Storm (Goldman, 1967; Darkow, 1969; Sasaki and Syono, 1966), which will eventually be applicable to all thunderstorms including Florida thunderstorms.

Since most of the present theories are based on knowledge of the environmental wind field throughout the depth of the storm, problems of adequate resolution in measurement of the atmosphere especially in the upper air will need solving. The forecasting problem however, can be approached in a pragmatic fashion by taking what information we have at hand and using it in the most effective manner. The tool that is available is radar, and, of necessity, we rely on radar to provide the needed motion data.

Intensity of the radar echo is also useful to determine the intensity of the system. From radar information given on a near continuous sampling interval (usually each 20 seconds), a history of the radar detectable storm is available and can be projected in space and time to provide the necessary axis along which the vertical wind profile is forecast to occur. The method of projecting the radar data forward in space and time has not been developed sufficiently for inclusion into the present numerical scheme. Present case studies are being used to derive empirical evidence of local storm motion characteristics. The combined results of these empirical studies will be incorporated in the numerical scheme.

7. References

Byers, H. R., and R. R. Braham, 1949: The thunderstorm. Washington, D. C., U. S. Government Printing Office, 287 pp.

Charba, J. and Y. Sasaski, 1967: Relations between the structure and movement of severe storms as revealed from mesonetwork data. Proc., 5th Conf. on Severe Local Storms, St. Louis, 238-245.

Darkow, Grant L., 1969: Deflecting forces of non-rotation convective systems due to environmental shear. To be presented at the Amer. Meteorol. Soc. Meeting in April, 1969.

Gerrish, H. P., and H. W. Hiser, 1965: Mesoscale studies of instability patterns and winds in the tropics. Report No. 8, Institute of Marine Science, University of Miami.

Goldman, J. L., 1967: A parameterized model of air circulation and rain distribution in severe storms. Final Report, NSSL, Contract No. E-36-67(N), ISR, Houston, 76 pp.

Goldman, J. L., 1968: The high speed updraft--key to the severe thunderstorm. J. Atmos. Sci., 25, 2, 222-248.

Goldman, J. L., and J. C. Freeman, 1966: The development of a model of air circulation and rain distribution in a steady state severe storm. Final Report, NSSL, Contract No. Cwb-11367, ISR, Houston, 55 pp.

Milne-Thomson, L. M., 1950: Theoretical hydrodynamics. New York, The Macmillan Co., 632 pp.

Sasaki, Yoshikazu and Sigekata Syono, 1966: Motion of the vortex with pressure and inflow which are not circular symmetry. No. ARL-1470-3, U. of Okla. Research Institute, Atmospheric Research Laboratory, Norman, Oklahoma.

6. EMPIRICAL OUTFLOW STUDIES

Joseph L. Goldman and Peter W. Sloss

In this study of the structure of the cold air outflow from thunderstorm cells, particular attention is paid to the dimensions and the speed of movement of the leading edge of the cold air. The boundary between environmental warm air and thunderstorm cold air is considered not a sharply defined surface but a zone in which there are steep gradients of wind and temperature. Details of the wind and temperature in the cold air, in the warm air near the boundary of outflow, and in the boundary zone itself, indicate smaller scales of variation than are usually considered in mesoscale.

Data sources for this study were radar stations at Daytona Beach (DAB) and Patrick AFB (COF), NASA's 150-meter meteorological tower (Fichtl, 1968, also Kaufman and Keene, 1968), and smaller towers of the Air Force "WIND" mesonetwork. Radar data consist mainly of photographs of the WSR-57 PPI scope at DAB, with about five minutes between frames. COF radar pictures, used mostly for verification, are Polaroid photos of the CPS-9 PPI taken at about 15 minute intervals. The ranges covered by the DAB and COF radars were 250 nautical and 75 statute miles, respectively.

The primary source of wind data for this study was NASA's 150-meter meteorological tower at Cape Kennedy, Florida. Time resolution of data from the tower is up to ten data points per second for wind speed and direction at each of seven measuring levels on the tower. Recordings

on this time scale were made intermittently, while analog strip charts ran continuously over a period of several months.

The analog strip charts may be interpreted on a minimum measurement interval of about two independent data points per minute (about 0.5 minutes apart). Analog wind records are considered to be readable to the nearest one m sec^{-1} in speed and five degrees in direction. The width of the ink line on the charts precludes resolution greater than 30 seconds. The one-tenth-second data are fully digitized and not subject to such difficulties, but the lack of these data in a convenient form at the time this report was prepared hindered detailed analyses.

The WIND mesonetwork data are only 30 minute averages, so much of the detail in the true wind field is smoothed. The wind shift line, in the 30 minute period, may move a distance several times greater than the spacing of the WIND towers. Caution must therefore be exercised against interpreting the WIND data as being more than a qualitative indication of the position of the wind shift line.

A. Data and Analysis

The analysis process consists of four principal activities:

a. identification of a wind shift at the 150-meter tower,

b. determination of the location and motion of the related radar echo,

c. time-to-space conversion of tower data, using echo velocity, and time-section plotting of isotachs,

isotherms, and isogons, and

d. combination of tower data with WIND network data for three-dimensional analysis.

Analysis of each storm begins with identification of a shift in wind direction accompanied by an increase in wind speed, as recorded on the analog strip charts. The radar picture for that time is then examined to determine the position of the echo nearest the tower, and the movement of that echo is measured from successive frames of the radar film. The point and averaged data for the wind shift period designated on the analog strip charts are plotted on time-sections. Spot data (where available) from the 0.1-second digital output are plotted and examined on time-sections. Temperature data are plotted on the time-sections of 0.5 minute analog wind measurements. The time record of winds from the tower are then converted into a spatial representation by assuming the thunderstorm outflow wind field to be quasi-steady and moving with the velocity of the echo (Fujita, 1963). The converted tower data are then plotted on a map along a line through the 150-meter tower and parallel to the echo velocity vector. This line of time-to-space converted data is then combined with mesonetwork data for further spatial definition. The combination of this "surface" of data with the WIND network data produces a three-dimensional representation of the wind field in and around an outflow front.

Precipitation and pressure measurements are two pieces of

information missing from the analysis scheme. No rain gage data were available to us, and the weekly pressure charts do not show a fine enough scale for our purposes. It is hoped that the unfortunate lack of rain gage data from locations near the KMT tower may be remedied in the future.

Temperature data from the tower and the mesonetwork were smoothed, which made the matching of tower temperatures with network temperatures difficult. Horizontal temperature distribution is therefore not shown.

B. Case Studies

The four storms discussed here occurred on 2 June and 17, 18, and 27 July 1967. Digital (0.1-second) data are available for the first and last cases. We shall consider the storm of 18 July in greatest detail because of the completeness of radar, mesonet, and analog tower data on that day. A complete summary of all data used appears in Table I.

The radar echo pattern for 1530 EST, 18 July 1967, is shown in Fig. 10. The location of the tower is indicated and the echo cell, assumed to be the source of the cold outflow measured at the meteorological tower, is heavily outlined and shaded in the drawing. Motion of this echo is from 230 degrees at 18 knots.

The winds passing the tower near the time of the wind shift were read from the analog records and plotted in a time cross section, and isotachs and isogons were drawn, as in Fig. 11.

Fig. 12 is the combined display of one-minute wind averages from

TABLE I

SUMMARY OF DATA

KMT Wind Measurements { A = Analog 1 minute average; D = Digital 0.1 second data } All times in GMT

Date		Wind Shift			Wind Speed Increase			Max. Recorded Speed			Max. Vertical Shear	
		Before	After	Start Time	Began	First Peak	Speed ($m\ sec^{-1}$)	($m\ sec^{-1}$)	Height	Time	(sec^{-1})	Layer
2 June 67	A	340°	290°	1550	1555	1602	22	22	120m	1602	0.2	3-60m
	D	(340°)	290°	(Before sample began)	(1555)	1600	16	22	120m	1602	0.5	18-30m
17 July 67	A	140°	260°	2025	2032	2037	12	12	120m	2037	0.2	3-60m
18 July 67	D	080°	360°	2013	2015	2017	12	18	90-150m	2020-21	0.3	3-30m
27 July 67	A	Analog Data Incomplete			----	----	--	--	------	-------	---	-----
	D	Being Processed by Computer-----Spot-Checked by Hand							------	-------	---	-----
11 June 68	D	Being Processed by Computer				----	--	--	------	-------	---	-----

TABLE I

KMT Wind Measurements--continued

Date		Max. Horizontal Wind Acceleration ($m\ sec^{-1}\ min^{-1}$)	Times	Level	DAB Radar Photo Time	DAB Radar Cell Movement From^0	DAB Radar Cell Movement at Knots	WIND Data Status	
2 June 67	A	6	1556-58	90 m	1558	345	10	NA	
	D	8	1557-58	60 m	----	(Tops	37 K)	Plotted	
17 July 67	A	4	2033	60 m	1947	250	20	Plotted	continued
18 July 67	A	6	2015-17	90 m	2030	230 (Tops	18 46 K)	Plotted	
27 July 67	A	-	----	---	----	Little	Movement	Plotted	
	D	Being Processed		---	----	---	--	------	
11 June 68	D	Being Processed		---	----	---	--	NA	

TABLE I

KMT Wind Measurements--continued

Date		Surface (3 m) Temperature: Before shift (^{0}F)	Max. dT/dt (^{0}F min^{-1})	After shift (^{0}F)	Mixing Zone Length (Kilometers)	Spacing of Wind Speed Maxima: Minutes	Kilometers
2 June 67	A	79	-2	69	2.2	5	1.1
	D	--	--	--	---	-	---
17 July 67	A	81	-1	73	4.9	4	2.5
18 July 67	A	82	-2	77	2.8	5	2.8
27 July 67	A	89	-1	84	Not calculated	Not calculated	
	D	--	--	--	---	-	---
11 June 68	D	--	--	--	---	-	---

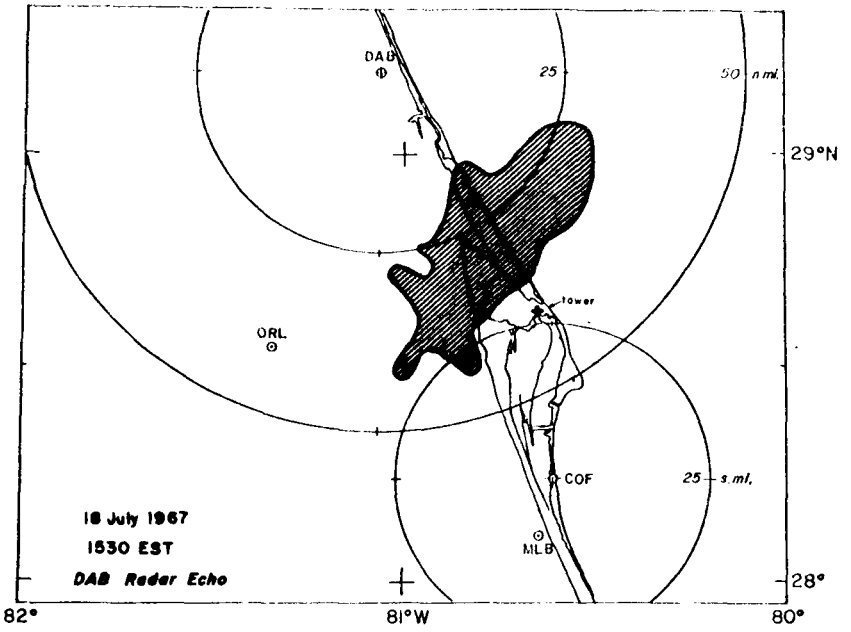

CAPE KENNEDY REGION

Fig. 10 Radar echo cell nearest the 150-meter meteorological tower as shown by Daytona Beach (DAB) radar. Echo tops were near 31 K in this cell. (Other echoes have been deleted for simplicity.) Movement of the cell was from 230 degrees at 18 kt; the slant of the hatching on the echo indicates that direction.

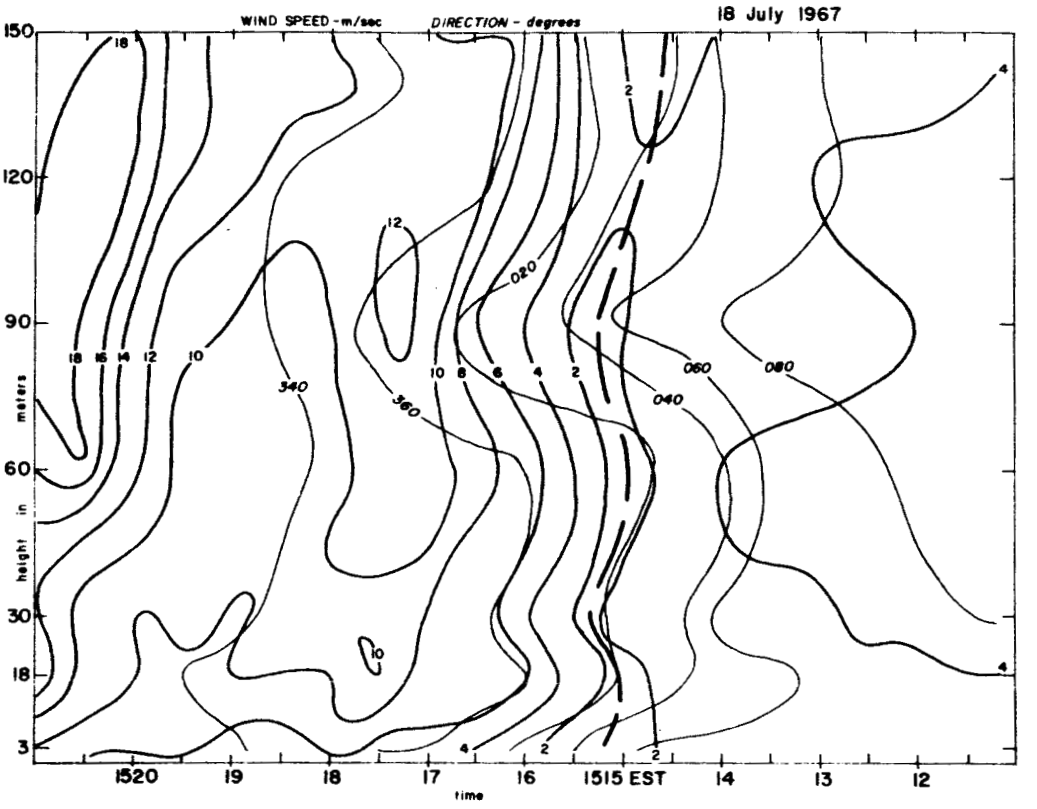

Fig. 11 Isotachs (dark-solid), isogons (light-solid) and isotherms (light-dashed) for storm of 18 July 1967. Heavy broken line is absolute wind speed minimum.

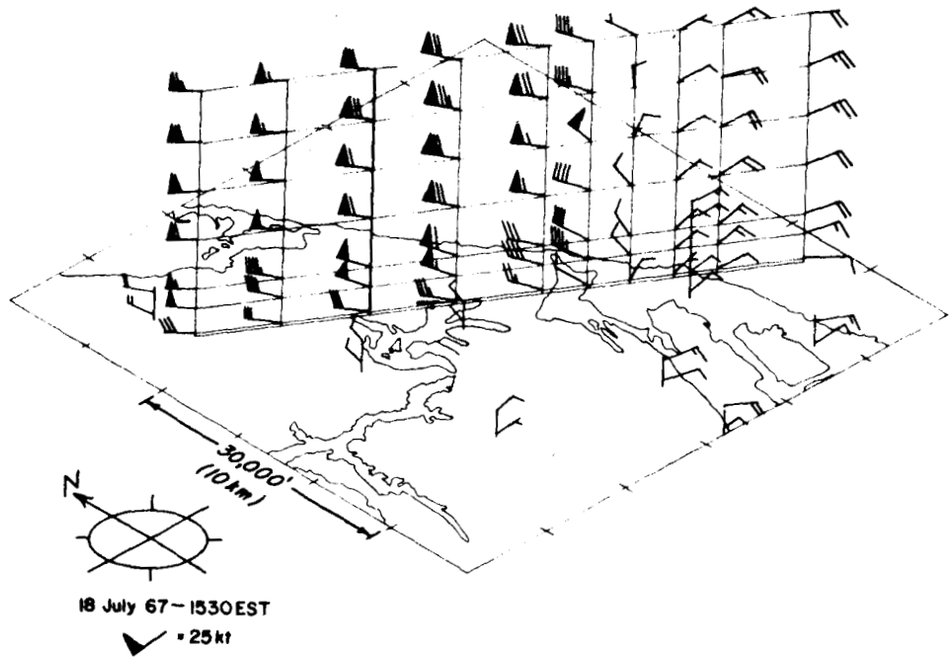

Fig.12 Detail of the Kennedy Space Center near the 150-meter tower (heavy vertical line) showing part of the "WIND" mesonetwork (shorter tower symbols). The slanting grid contains wind flags for one minute averages of tower analog data; vertical grid lines are five minutes apart and represent a height of 150 meters. The "WIND" towers report 30 minute averages.

the analog data (with time-to-space conversion plotted as wind flags on the slanting grid) and the mesonetwork wind data (plotted on an oblique-projection map of Cape Kennedy). The map projection was drawn so as to preserve parallel lines on the ground. On the map the meteorological tower and the mesonetwork stations are located with a vertical scale exaggeration of about 50:1, so that the vertical distribution of the wind field may be seen clearly.

Fig.13 is a plot of the continuous temperature records for each level on the 150-meter tower. The sharp drop in temperature at all levels accompanies the first wind speed maximum after the wind shift. The isotherms displaying this temperature drop are shown as the light dashed lines in Fig. 11.

The data from the 18 July storm show strong evidence that the cold air is nearly isothermal in the lowest 150 meters, having a vertical lapse rate of about 0.5 F per 150 meters (Fig.11). There is a horizontal temperature difference of 6 F from the warm air passing the tower at 1515 EST and the cold outflow air passing the tower at 1521. At 1517 there is a maximum horizontal temperature gradient of nearly 1 F in 150 meters. The steepness of the temperature drop, as shown in Fig.13, is maintained only over a short interval near the forward edge of the advancing cold air. The isotherms in Fig.11 show that the cooling from the leading edge of the cold air extends farthest downstream at the highest tower level. There is an extreme forward tilt of the 82 F isotherm not seen in the cooler isotherms

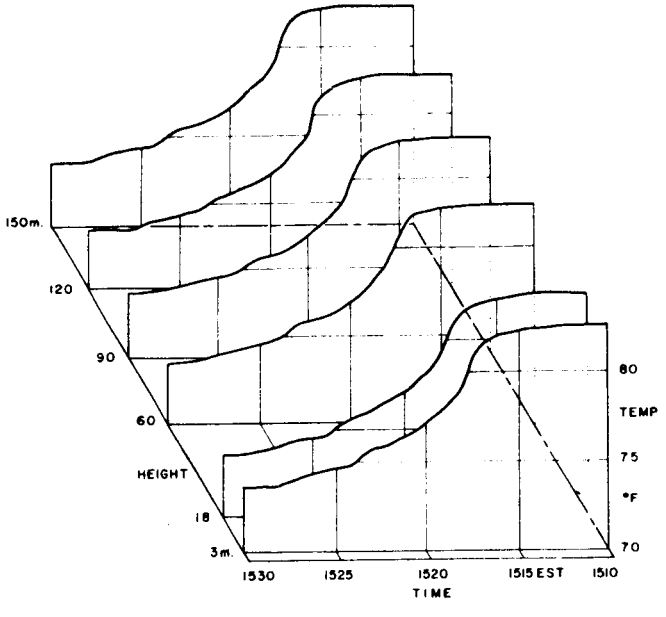

Fig.13 Temperature profile measured at the 150-meter tower during passage of the cold air outflow.

behind it, but all isotherms do slant downstream as they extend upward.

Fig.11 indicates a sharp velocity gradient just ahead of the edge of the cold air, but it appears that the gradient there is produced as the cold air pushes the warm air out of the way. The heavy broken line in Fig.11 marks the minimum in wind speed just ahead of the cold air where the flow changes from warm ambient conditions to cold storm outflow. The fact that the temperature drop lags over 1 km behind the change in the flow pattern may be indicative of mixing at the leading edge which causes the maximum temperature gradient to move farther back into the cold air. The mixing is greatest where the velocity gradient is greatest; hence, the temperature gradient should be greatest where the velocity gradient is the least.

Change of wind direction before increase in speed has been noted previously (cf. Fig. 46 in Byers and Braham, 1949), from data from a multilevel meteorological tower. The observations presented here contain much more detail of the horizontal and vertical structure of the outflow near the ground. In particular, we can see that wind direction change begins in warm air and wind speed increase occurs in cold air. For our 18 July case the separation between the direction change and the first wind maximum (which accompanies the temperature drop) is about 2.5 km. Another 6 to 7 km separate the recorded temperature minimum from the wind maximum. Thus, the total horizontal extent of the warm air-cold air mixing

zone must be around 7 to 9 km along the direction of movement of the cold air. In the case under discussion the time needed for conditions to change from pure warm air to pure cold outflow air is 15 minutes.

The wind direction changed from just north of east to due north in about five minutes. Sixty degrees of the direction change in the lowest 60 meters occurred while the wind speed was decreasing to its absolute minimum. At higher levels, the direction change was closer to 40 degrees before the speed minimum. At all levels the rate of change of direction is greatest near the speed minimum.

The spacing of wind speed maxima in the region behind the outflow front indicates eddies of 2.8 km on the scale and a period between maxima of about 5 minutes.

Also included in the data sample for this study, beside storms on 2 June and 17 and 27 July 1967, was the storm of 11 June 1968. Wind data for the 27 July 1967 and 11 June 1968 cases are available to us as digital KMT data on magnetic tape and on 400 foot rolls of paper. Difficulties in using the tapes have delayed detailed analysis of available data, but a limited spot-check has been made for the 2 June and 27 July data from the paper rolls. WIND network data are available for the 27 July 1967 case, but no time-to-space conversion has been done because the radar echo did not appear to move. A time-to-space conversion was made for the 17 July 1967 case, but, due to some radar malfunction, it is based on echo movements at approximately 45 minutes before the wind shift at the

tower. We will discuss the 2 June and 17 and 27 July cases in chronological order.

Both analog and digital KMT wind data are available for the 2 June case. The WIND network data did not begin until 14 June and so are not available; the time-to-space conversion was therefore done but not plotted on a map. Daytona Beach radar PPI shows an echo cell immediately adjacent to the KMT at 1058 EST (1558 GMT). Position and movement of the echo are indicated in Fig. 14.

The KMT analog data show the wind shift began on 2 June about 1550 GMT (exact details are masked by calibration marks on the strip charts); our data sample begins at 1555 GMT. Wind speed is plotted in Fig. 15 and direction in Fig. 16. The increase in wind speed lags more than five minutes behind the change in direction, and the first peak in wind speed appears about ten minutes after the shift.

It should be noted that the radar echo on 2 June was moving at only 10 knots, or little more than half the speed of the 18 July echo analyzed above. There is a longer time span from wind shift to first speed peak on 2 June, but the speed of the storm is such that the corresponding distance between the wind shift and speed maximum is nearly the same for the two storms.

The KMT digital data were analyzed from the printed output but only a spot average was applied to the data, i.e., a two-second average at the beginning of each minute. (More complete use of the digital data

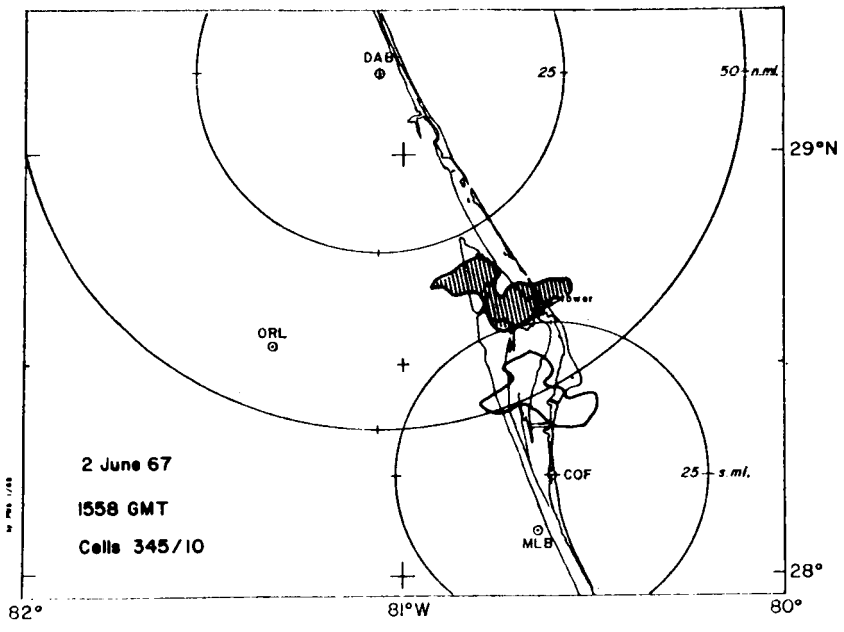

CAPE KENNEDY REGION

Fig. 14 Daytona Beach Radar PPI. Hatched echo is source of outflow.

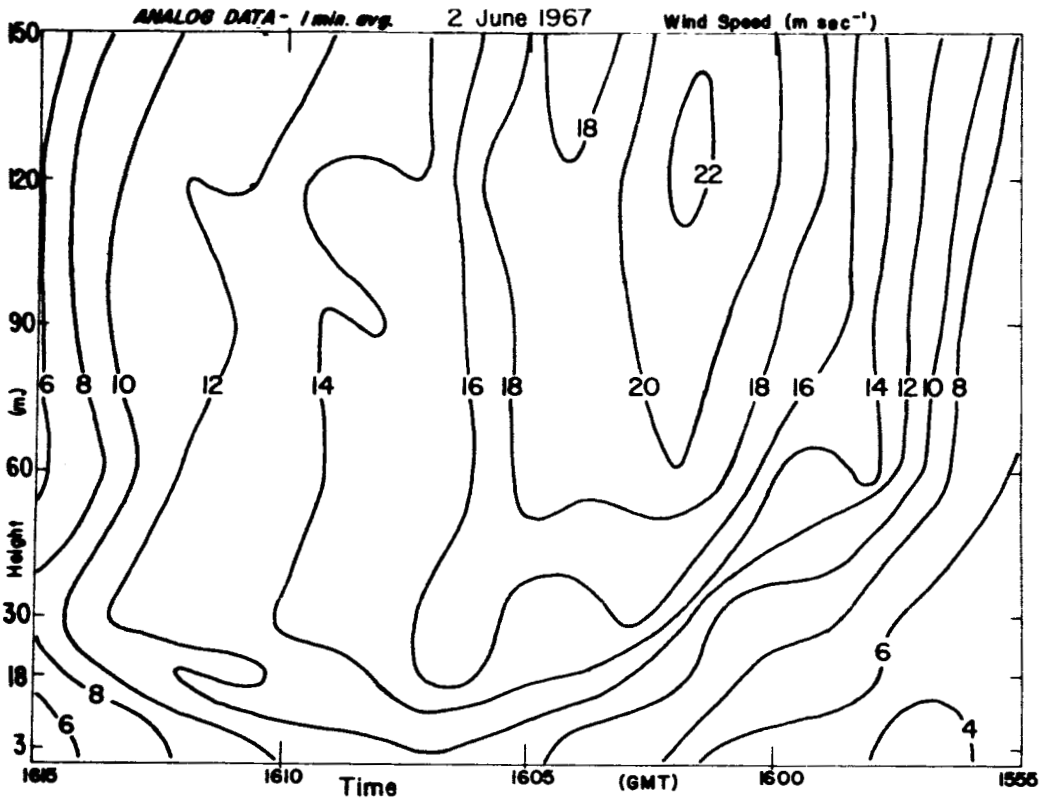

Fig. 15 Isotachs from 2 June 1967. Analog KMT data.

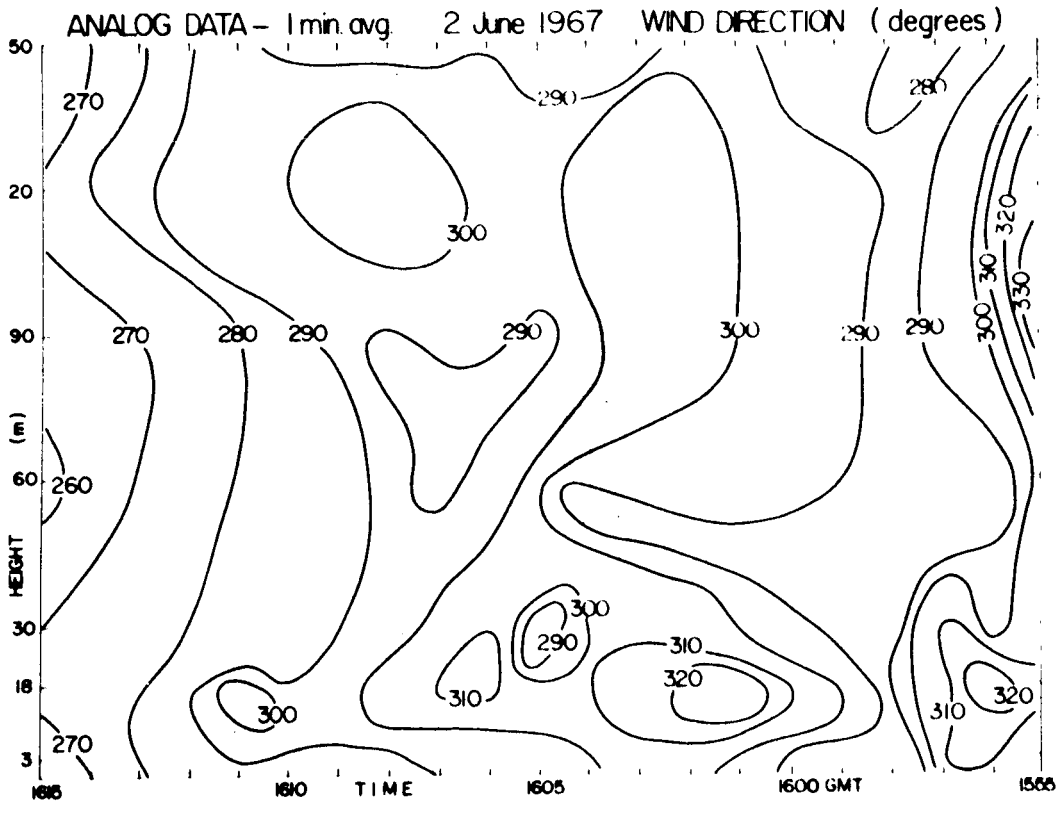

Fig. 16 Isogons from 2 June 1967. KMT analog.

will be made shortly when the magnetic tapes are processed by computer.) Wind speeds taken from the KMT digital printout are shown as isotachs in Fig.17. Note that the digital data start at 1557 GMT, the beginning of the sample on the tape.

A comparison of Figs. 15 and 17 shows that the same features appear in both presentations. There are some differences between the two plots of wind speed where gradients are large. The digital data show a maximum horizontal velocity gradient of 8 m $sec^{-1} min^{-1}$ in the one minute from 1558 to 1559 GMT while the larger averaging period applied to the analog data spreads the gradient out over two minutes with a maximum of 6 m $sec^{-1} min^{-1}$. Vertical shear of velocity exceeds 0.5 sec^{-1} between 18 and 30 meters height in the digital data. It is hoped that further processing of the magnetic tape will reveal other important structures in the flow.

Temperature data at 3 meters height show a 9 F drop, starting at 1555 GMT or about five minutes after the direction began to shift. The gradient of temperature shows the same dependence on velocity gradient as was seen in the 18 July data, i.e., large velocity gradients are concommitant with smaller temperature gradients. No vertical cross section of temperature could be made from the data.

The storm of 17 July 1967 is not as well documented as some of the others. Radar data are incomplete and cell movement from 250 degrees at 20 knots is estimated from pictures taken 45 minutes before the

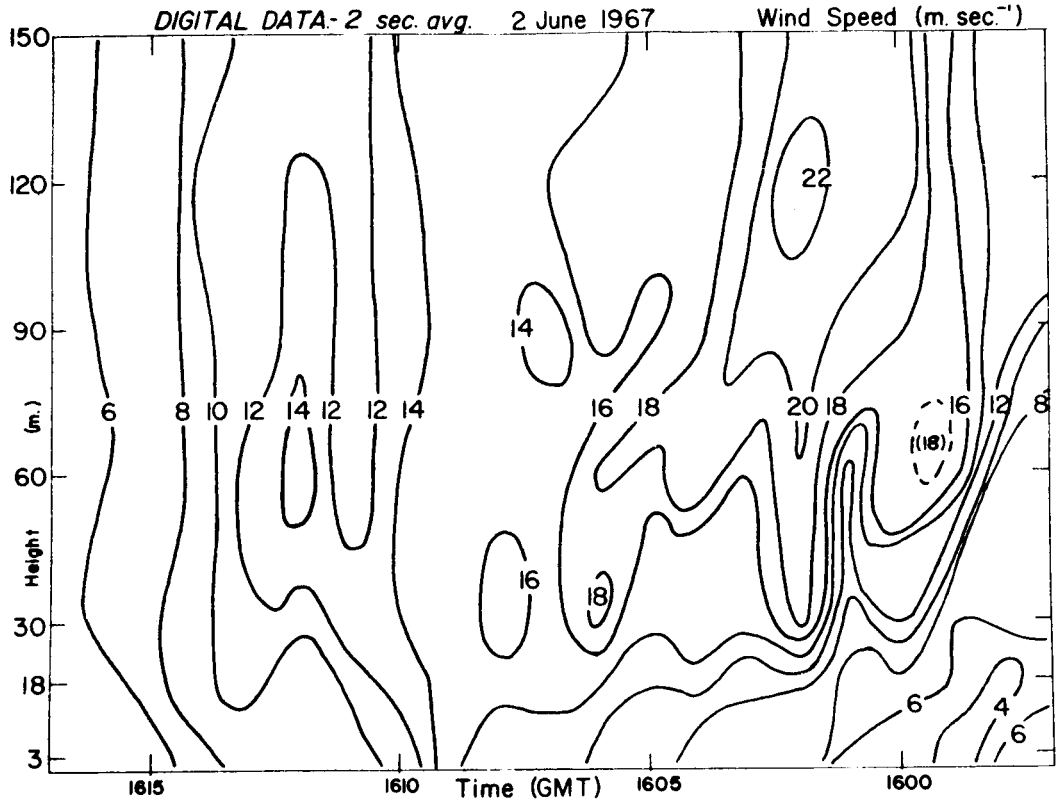

Fig. 17 Isotachs from 2 June 1967. Digital data.

storm passed the KMT. No echo map has been drawn because of the lack of proper data.

Qualitative features of this case are summarized in Fig.18, which shows the passage of the outflow front in isotachs and isotherms and Fig.19, a time-to-space conversion based on the estimated storm movement. Note the disparity in Fig.19 between the KMT 1-minute analog winds (heavy wind arrows) and the WIND 30-minute averaged winds (lighter wind arrows).

The wind shift occurred at 1527 EST, changing 120 degrees in two minutes. Isogons were not plotted because the wind direction was highly variable during the wind speed minimum (1525-30 EST); however the shift can be seen clearly in Fig.19.

The temperature structure in the 17 July case shows stronger vertical temperature gradients than on 18 July. There is a noticeable upstream slant to the isotherms in Fig.18 below 30 meters. Fig. 20, a time-height-temperature composite for 35 minutes of data, shows two steep temperature gradients correspond to the two peaks in wind speed.

The peak winds for the 17 July storm were weaker than for the other cases discussed here, and the gradients of velocity are correspondingly less. Maximum wind speed and horizontal and vertical shears are about half what was measured on the other cases.

We had hoped to include a discussion of the 27 July 1967 and 11 June 1968 storms, but delays in processing the magnetic tapes prevent

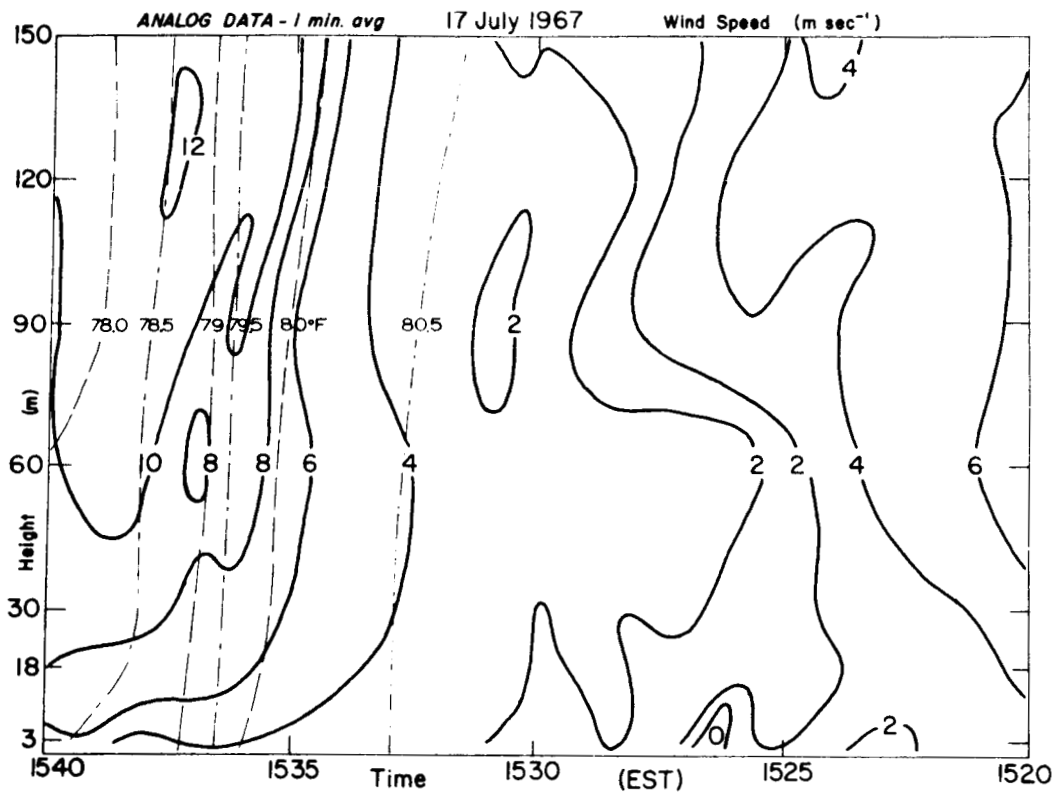

Fig. 18 Isotachs and isotherms for 17 July 1967. KMT analog data. Isogons have been deleted to avoid overfilling the page.

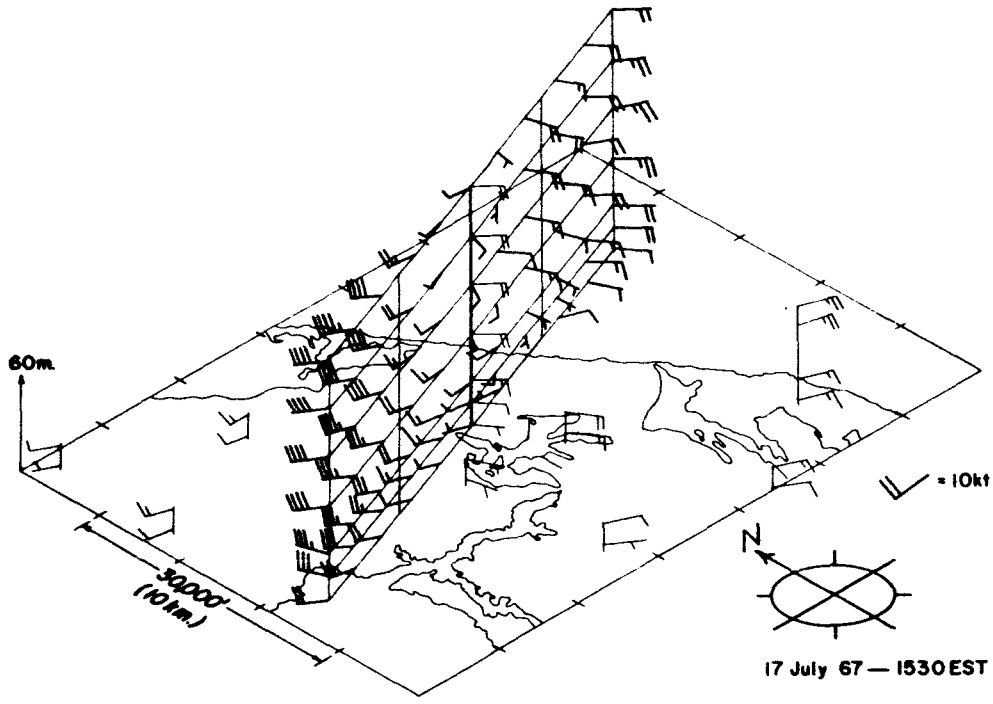

Fig.19 Time-to-space conversion of 17 July 1967. KMT analog and WIND network data (based on echo movement 45 minutes before indicated time). Note disparity between KMT analog one minute averages (dark flags) and WIND network 30 minute averages (light flags). Vertical grid lines are five minutes apart.

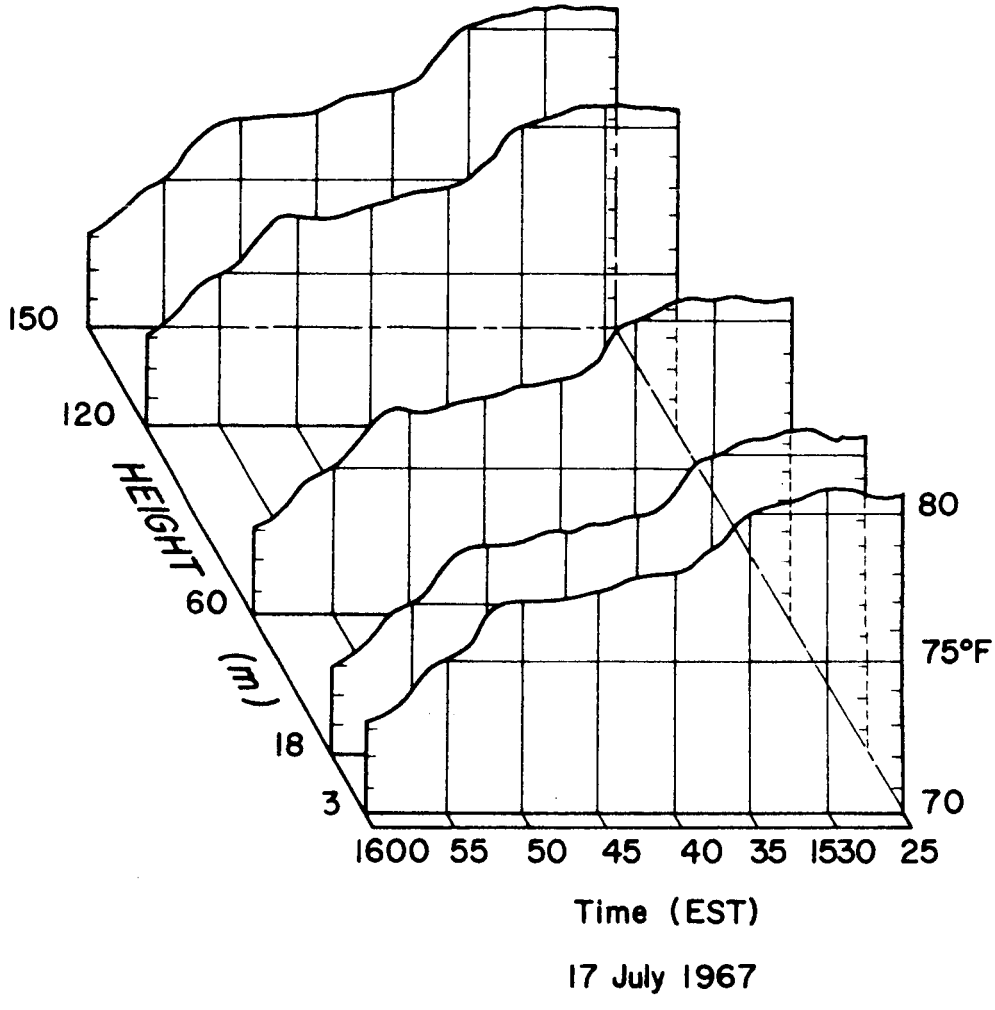

Fig. 20 Time-height-temperature plot for 17 July 1967.

us from doing so. The 27 July storm, which was stationary with strong outflow winds, should provide a measure of the mass flux of the outflow without the effect of the storm's motion. It may then be possible to go back to the other cases to determine their mass flux and correct for the motions of the storms.

C. Relation of the Outflow to Hydrodynamic Barrier Flow

The principal finding of this study is that there is a striking similarity between measured storm outflow patterns and the flow of fluid around a bluff body. This flow is usually modeled by a source of fluid in a uniformly moving environment. When the thunderstorm outflow is represented by the source flow and the sea breeze environment represented by the uniform stream, a streamline pattern should be seen that strongly resembles the wind patterns in Figs. 12 and 19.

Hydrodynamic models usually provide for a streamline which divides the two flow regimes. It appears that, in nature, this boundary is somewhat eroded by turbulent exchange between the warm environment and the cold outflow. The temperature structure shows that there is a zone about 5 to 10 kilometers wide in which the flow changes from ambient warm air to cold outflow air.

Our data only extend down to 3 meters off the ground so we cannot make definitive statements about the ground surface boundary layer, but in the layer between 3 and 30 meters there is a lag of some 0.5 to 1.5 km between the arrival of a particular isotach at 30 meters and the appearance

of that speed at 3 meters. Direction changes also propagate downward through this layer. No such strong tilt is seen in the isotherms between 3 and 18 m but the gradient is stronger at the lower levels in the cold air. (No thermocouple was located at the 30 meter level.)

Multiple wind maxima are seen at all tower levels in each storm. Maxima occur at about 5 minute intervals regardless of the speed of the storm echo. This periodicity is seen even in the 27 July storm, which had a stationary echo.

The spacing of wind maxima and the length of the mixing zone may be somewhat arbitrarily scaled by the component of the mean outflow wind along the direction of echo motion. This scaling has been applied to the data (rather crudely) to generate the last two columns in Table 1. This approximately five minute periodicity of the wind maxima seems to be a common feature of the wind data and thus should warrant further investigation.

D. Summary and Conclusions

It is certain from the data we have seen that the structure of the cold air outflow wind field is quite different from the normal sea breeze environment present on Florida's East Coast on a summer afternoon. The cold outflow wind field pours out from the storm, intruding into the ambient flow pattern. The manner of change in wind velocity before, during, and after the passage of the edge of the outflow is similar to

hydrodynamic barrier flow. The length of the mixing zone at the leading edge of outflow is about 5 to 10 km.

Nothing has been said about the motions of wind maxima within the cold air relative to the leading edge. Since these motions are of the scale of eddies, inferences will be drawn from detailed analyses which are now in progress. For the purpose of this paper, the outflow moves with the storm. We can state that the leading edge of the cold air mass from the storm has a nearly vertical front (in the lowest 150 meters), as evidenced by the temperature field, and that the wind field is definitely influenced by the ground surface.

E. References

Byers, H. R., and R. R. Braham, Jr., 1949: The thunderstorm. Washington, D. C., U. S. Government Printing Office, 287 pp.

Fichtl, G. H., 1968: Characteristics of turbulence observed at the NASA 150-meter meteorological tower. J. Appl. Meteorol. 7, 838-844.

Fujita, T., 1963: Analytical mesometeorology: a review. Meteorological Monographs, 5, 77-128.

Goldman, J. L. and P. W. Sloss, 1969: Structure of the leading edge of thunderstorm cold air outflow. Submitted to 6th Conference on Severe Local Storms, Chicago, April 8-10, 1969.

Kaufman, J. W., and L. F. Keene, 1968: NASA's 150-meter meteorological tower located at the Kennedy Space Center, Florida. NASA TMX-53699.

7. WIND DIRECTION OSCILLATIONS IN THE FLANK OF THUNDERSTORM OUTFLOW

T. Ushijima

Atmospheric waves have been reported in meteorological research within the range of 10^4 km maximum to 1 km minimum. We do not find scientific reports concerned with wave lengths shorter than 1 km. It may be that this lack of information is due to the low vertical height of the installation and lack of sensitivity of the usual wind recording instruments used in the research. Information from the 150-meter meteorological tower at Kennedy Space Center appears to indicate that variations in wave length are reduced by friction at ground level, because in the following case the oscillations recorded at the tower were not discovered by instruments at ground level. These five second oscillations, found in this case to be on the flank of thunderstorm outflow, will be analyzed and discussed from a gravitational point of view and compared with Faller's theory on large eddies and the Ekman-Taylor theory of the boundary layer.

A. Meteorological Conditions

A cold front extending from an occluded front emanating from a low pressure center at the Great Lakes was located near the base of the Florida peninsula on 9 May 1967 (Fig.21). The polar jet stream meandered about the low aloft, bringing it southward over Georgia. Locally the cold front passed Daytona Beach, Florida, at 0738 EST, 9 May with no rain, a

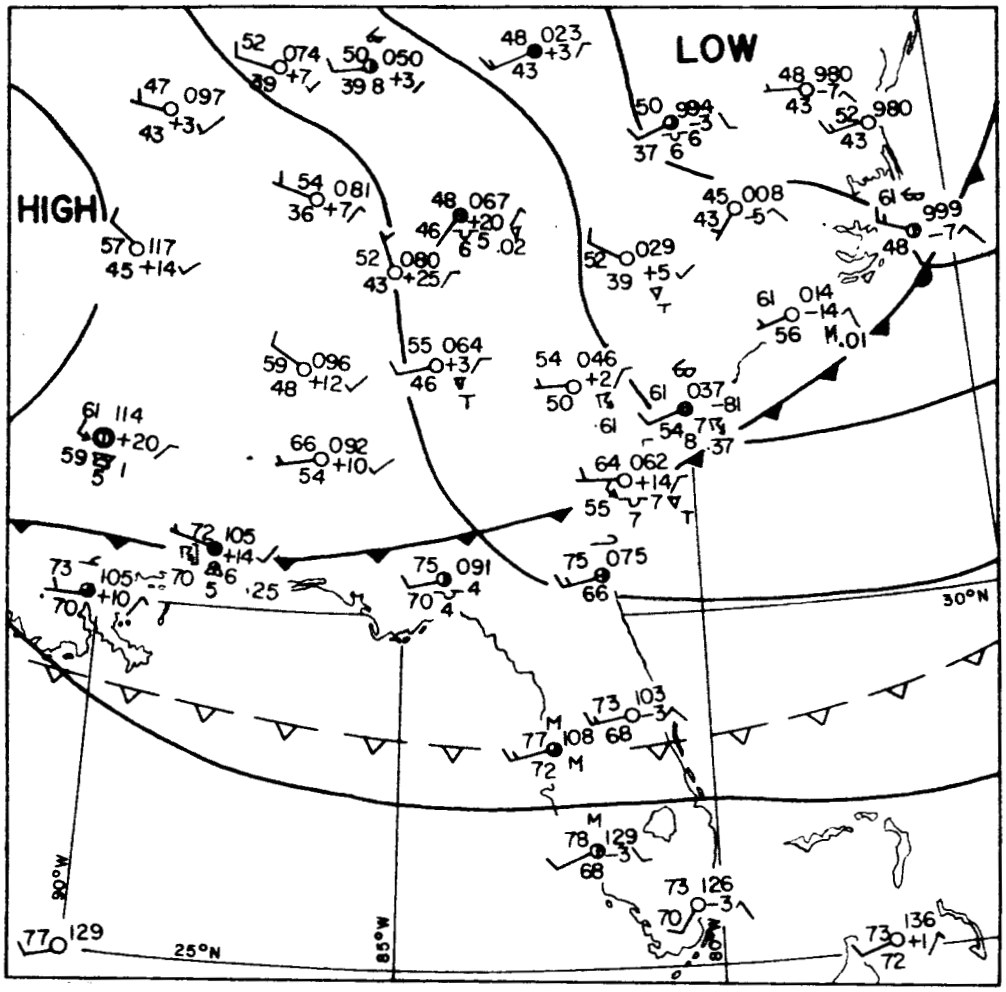

Fig. 21 Surface map for 0100 EST, 9 May 1967
▽ ▽ ▽ Location of cold front at 1300 EST, 9 May 1967.

temperature drop of 13 degrees Fahrenheit with a recovery after about one hour, humidity change of 45 per cent, and a wind shift of 60 degrees.

Photographs of the Daytona Beach radar contain a line distribution of echoes along the cold front. Although the line moved southeastward, individual cells moved east-southeast (285 degrees) at a speed of 35 km per hour. The nearest echo approached the tower at about 0910 EST. An estimate of the height of the echo top was 15 km, indicating that the cell was in the mature stage (Fig.22). If we consider the oscillation to be eddies moving at the speed of the line echoes, 35 km per hour, the size of these eddies are about 50 meters in diameter.

The front, as shown in Figs.23 and 24, passed the tower site at 0918 EST. However, it should be noticed that the fluctuation of the wind direction started at 0910 EST, eight minutes before the echo passed the tower.

Upper air measurements were taken with radiosondes at Cape Kennedy AFS, Florida, (about 10 nautical miles southeast of the tower) at 0638 and 1816 EST. According to the synoptic scale analysis a large temperature drop, which normally accompanies an active cold front, did not occur (Fig.25). Also, the temperature lapse rate in the layer below 975 mb (1000 ft) is nearly dry-adiabatic. This low stability and high wind speed at 0638 EST are indicative of a low-level jet below approximately 1000 ft.

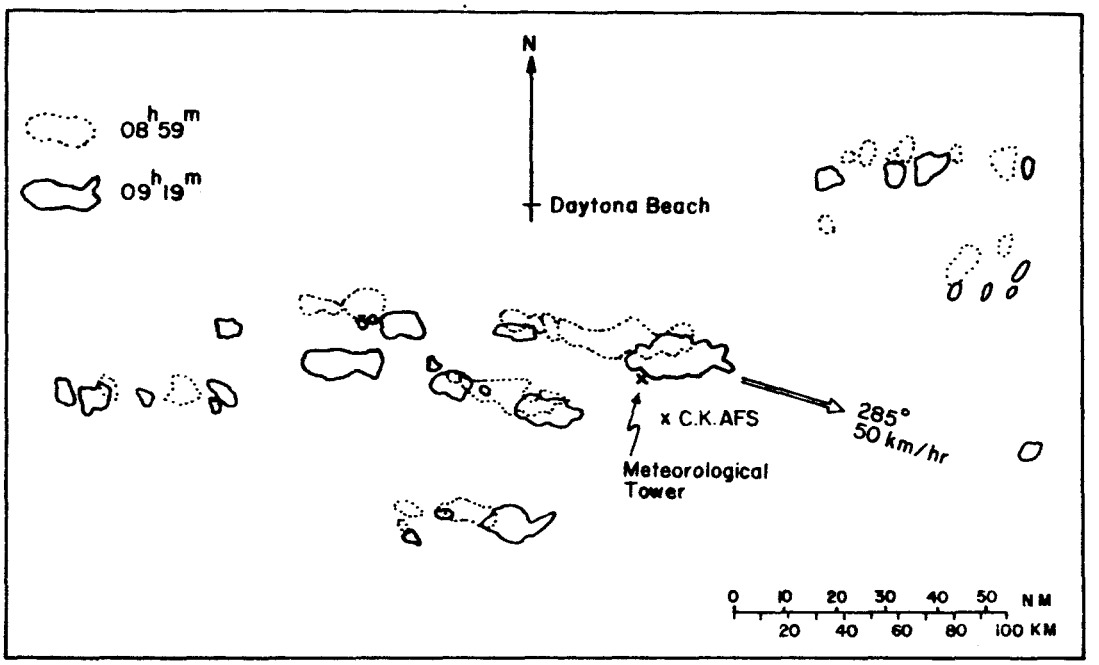

Fig. 22 Radar echoes distribution at 0859 EST & 0919 EST, 9 May 1967.

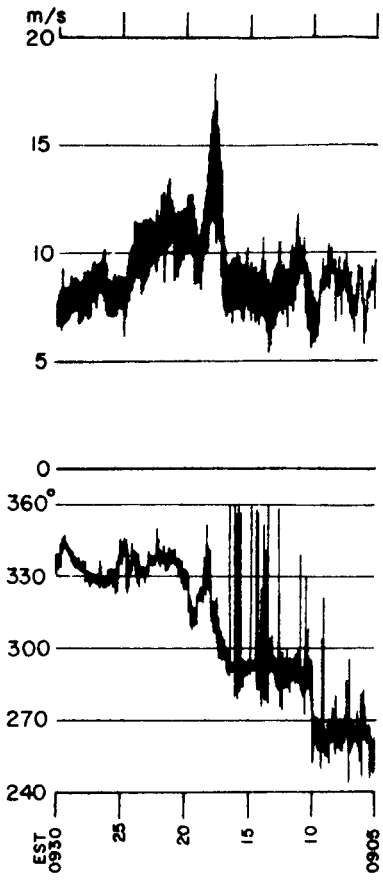

Fig. 23 Paper strip charts for wind speed (upper) and wind direction (lower) at the 120 m level.

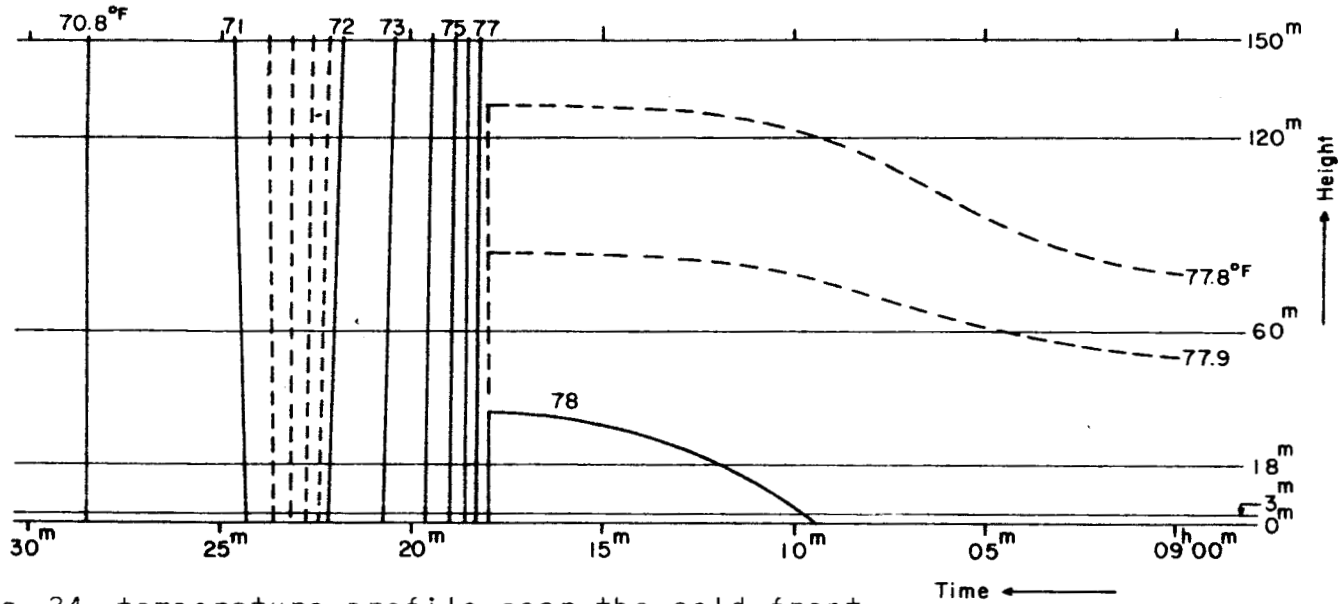

Fig. 24 temperature profile near the cold front.

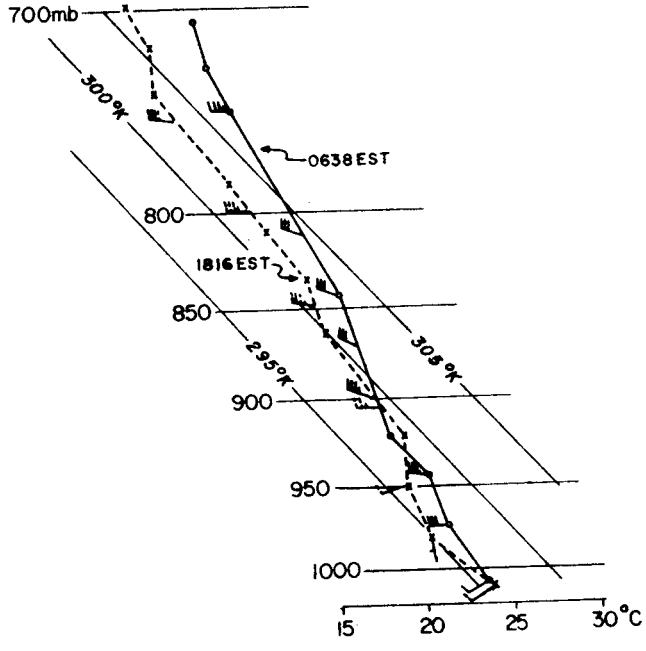

Fig. 25 Upper soundings at Cape Kennedy AFS, 0638 EST & 1816 EST, 9 May 1967.

B. Features of Oscillations

Because of the short-period character of the oscillations, both the response time and other characteristics of the instruments, which are installed on the meteorological tower, are critical. The data used were from the Climet Series Cl-14 instruments for wind observation at the 18, 30,60,90,120, and 150 meter levels. (Digital data did not include wind direction from the anemometer at 3 meters.) Dennis (1965) reported that fairly good wind data can be obtained up to gust frequency of 3-5 cycles per second by these sensors.

The thermocouples were installed also at the 3, 18, 60, 120, and 150 meter level. Temperature was recorded on strip charts with resolution of 25 seconds. Wind data were also recorded on strip charts with resolution of one-half minute, in addition to being digitized at 0.1 second intervals.

Although six cases of thunderstorm outflow in 1967 and 1968 were examined for these oscillations, only one case, 9 May 1967, was found to include the systematic oscillation.

The oscillation began at 0909 and 40 seconds EST, and continued to 0930 when the records were interrupted. As shown in Fig. 26 there is an increasing phase lag in the wind direction with height. For example, at 0909 and 42 seconds, a wind direction of 300 degrees appeared on the 90 m level first and then rose up to the 150 m level. The weak wind zones (below 6 m per second) correspond to the northerly wind on the 90 m level and the strong wind zones (above 8 m per second) exist below the weak wind zones

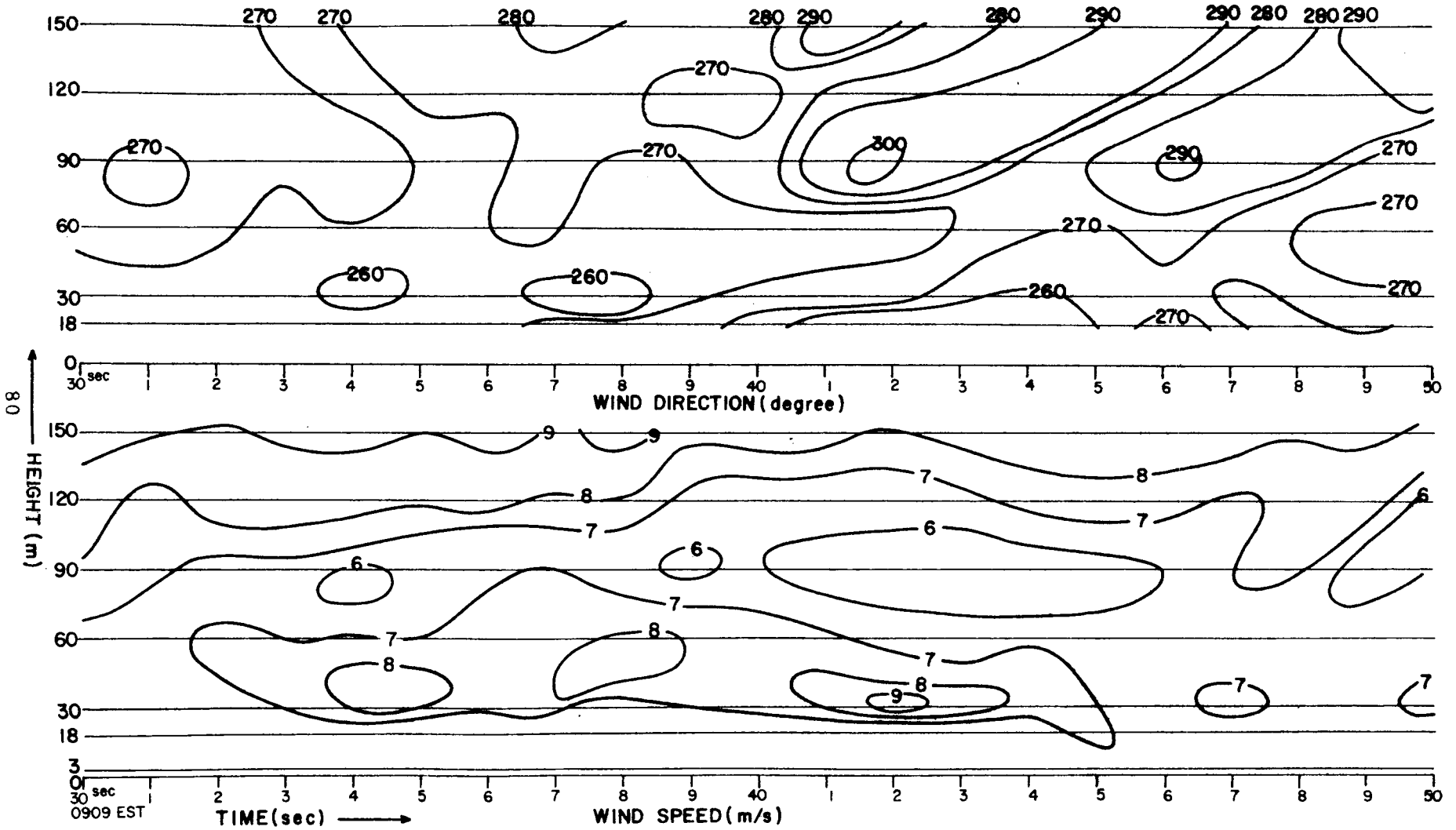

Fig. 26 Time sequences of wind direction (upper) and speed (lower) near the beginning of the oscillations

at 30 m. Fig.27 as well as Fig.26 shows the time sequences with raw values at every 0.5 second. The oscillations (Fig.27) are more clearly indicated than those shown in Fig.26, because they may be in the mature stage when the cold front or the cold outflow of thunderstorm passed the tower site.

The same trend as seen in Fig.26 can be found in Fig.27, except that the strong wind zones appeal in the 60 m level. The passage of the cold front produces a change of wind direction from easterly to northerly and increases the wind speed (Fig.27).

C. Discussion

The main observation to consider in this paper is the short period oscillations, but the unusual profile of the wind speed is also of interest. The oscillations occurred in both warm and cold air. The strong wind in the lower layer, when considered in profile, deviates from the normal Ekman spiral. Any speculation made to explain these measurements must satisfy both of the facts presented above.

First, one source of oscillations in the atmosphere is the internal gravity wave. When condensation occurs, gravity waves quite often appear in the form of billow clouds or lee waves. Their wave lengths (observed by the eye or radar) are of the order 1 to 10 km (Ushijima, 1959; Hicks and Angell, 1968).

The shorter the wave length, the smaller the vertical displacement.

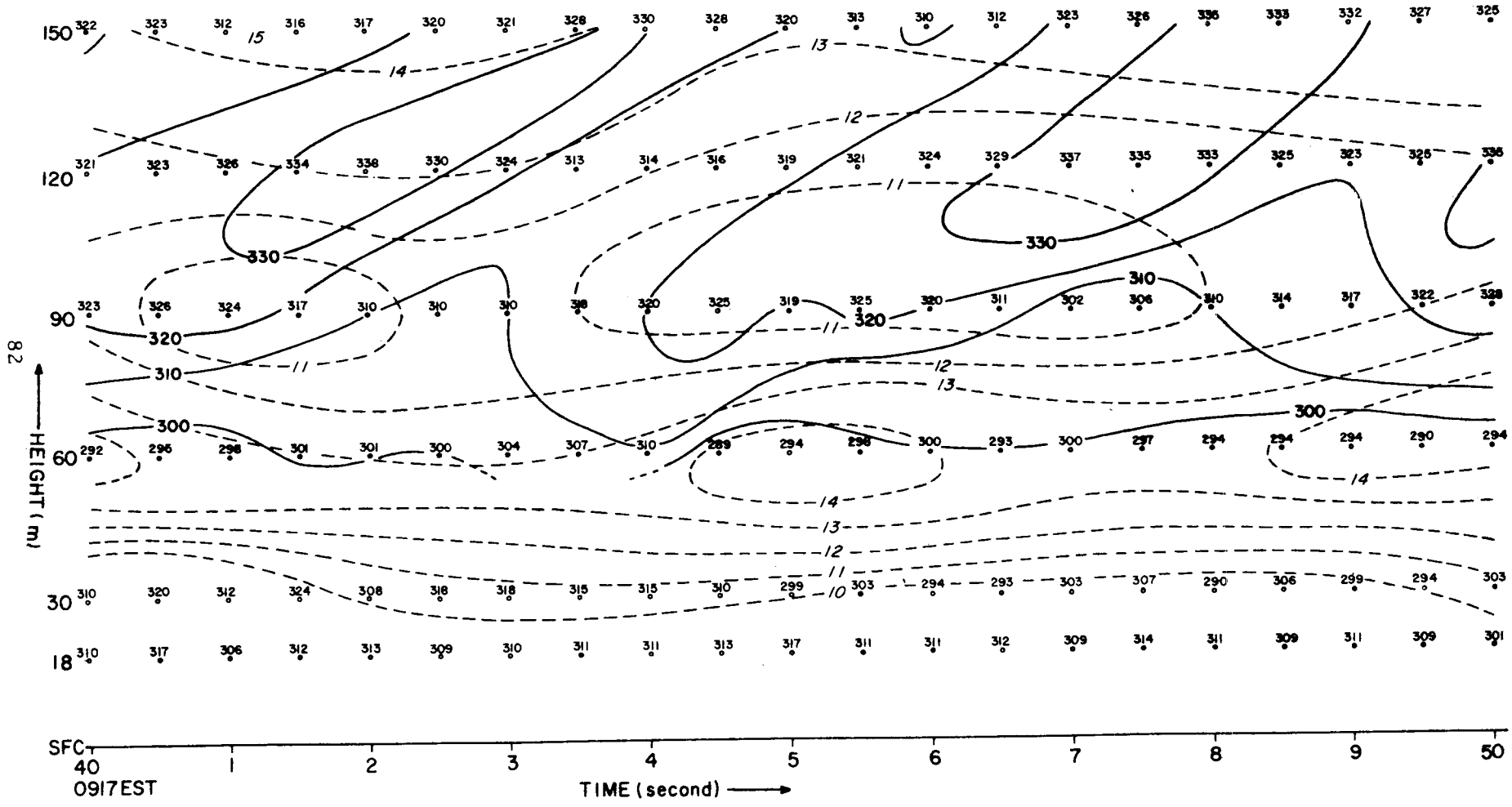

Fig. 27 Same as Fig. 26, but at the mature stage

Although gravity waves with lengths below 1 km have not been reported in meteorological literature, there is no reason why such waves cannot exist.

The phenomena discussed here have many of the properties of a very short gravity wave. This wave is usually on an interface between fluids of different densities. The velocity of the internal gravity wave can be represented by an advective term plus or minus a dynamic term.

More precisely, phase speed c of the shear-gravity wave in deep-water (see Ushijima, 1959, for one in shallow water) is

$$c = \frac{\rho u + \rho' u'}{\rho + \rho'} \pm \left[\frac{gL}{2\pi} \frac{\rho - \rho'}{\rho + \rho'} - \frac{\rho\rho'(U - U')^2}{(\rho + \rho')^2} \right]^{1/2} \tag{1}$$

where the densities of the lower and upper layers respectively are ρ and ρ', the velocities U and U', g the acceleration of gravity and L the wave length.

The c should be negative when the wave propagates upwind, namely, toward the cold air,

$$\frac{\rho u + \rho' u'}{\rho + \rho'} < \left[\frac{gL}{2\pi} \frac{\rho - \rho'}{\rho + \rho'} - \frac{\rho\rho'(U - U')^2}{(\rho + \rho')^2} \right]^{1/2} \tag{2}$$

Assuming U is U' as an extreme case,

$$U < \left[\frac{gL}{2\pi} \frac{\rho - \rho'}{\rho + \rho'} \right]^{1/2} \tag{3}$$

An application of the values at Cape Kennedy AFS yield approximately

$$U < 3\ ms^{-1}$$

under the condition as follows:

$$L: \quad 10\ ms^{-1} \times 5\ sec \sim 100\ m = 10^2 m$$

$$\rho: \quad 1080\ gr\ m^{-3}\ (3000\ ft\ level) \approx 1.1 \times 10^3\ gr\ m^{-3}$$

$$\rho': \quad 1017\ gr\ m^{-3}\ (5000\ ft\ level) \approx 1.0 \times 10^3\ gr\ m^{-3}\ .$$

The wind speed U actually was greater than $10\ ms^{-1}$. Accordingly, the waves could not proceed upwind. Since oscillations were also observed in the cold air, the waves might occur on the shallow cold-dome first, then propagate into both the warm and the cold air (Fig. 28). Perhaps the 5 second oscillation is found only on the flank of the cold air, and not at its leading edge. Gravity wave theory, which allows for measured variations of the wind direction, does not allow for the observed strong wind in the lower layer.

Faller's theory (1965), which can be adapted to the existence of the large eddies in bands, agrees with some of the above observations, especially with respect to the strong wind zone in the lower layer (see Fig. 29, 0638 EST profile). However, observations show these waves moved very fast, while according to Faller the bands should be nearly stationary.

It may be interesting to consider the abnormal velocity profile as a problem of the Ekman-Taylor boundary, apart from the oscillations, since

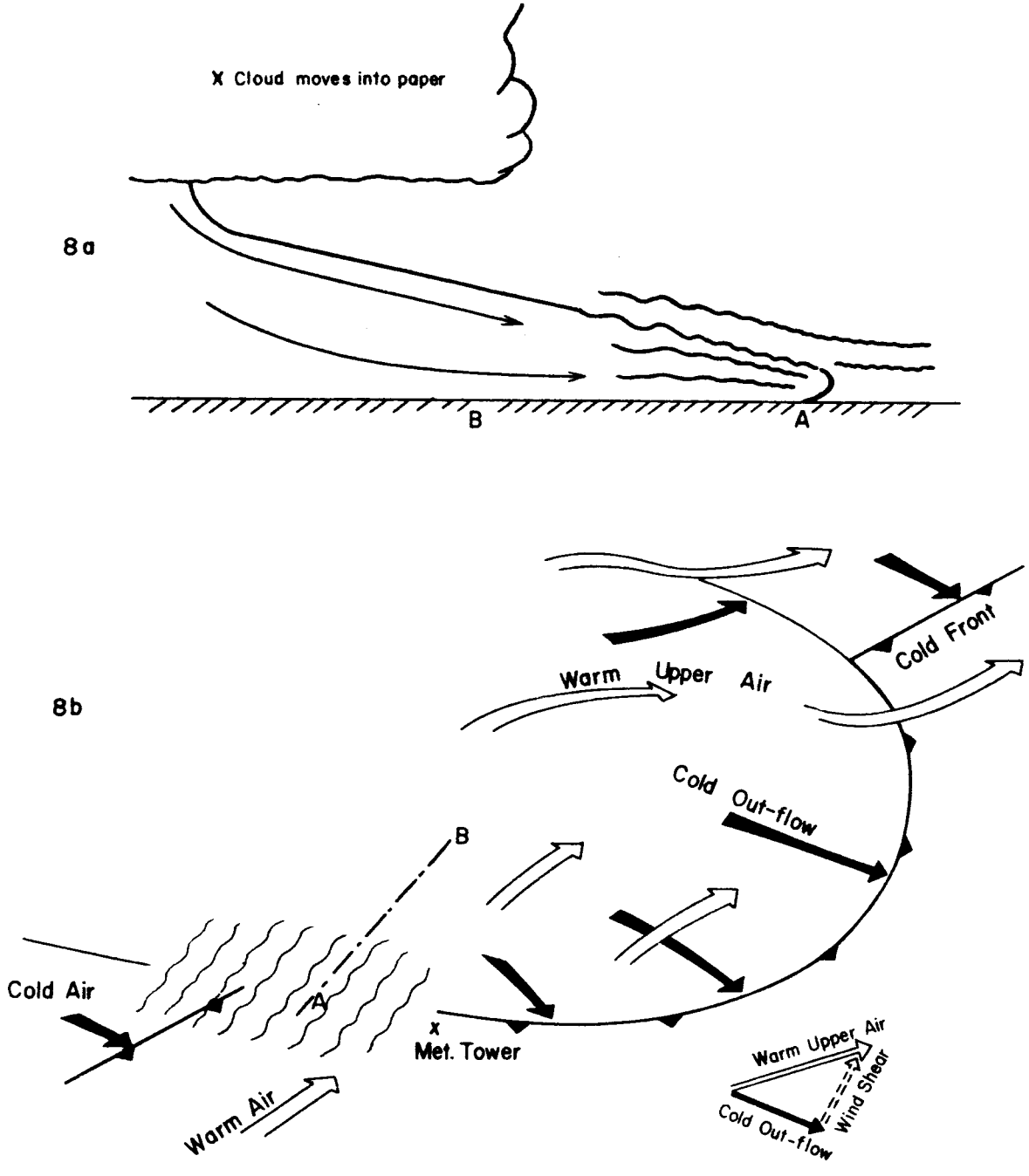

Fig. 28 A model illustrating the source of gravity wave.
(a) Side view of storm cloud and outflow.
(b) Perspective view of outflow and wind field. Point A and B correspond in the two figures.

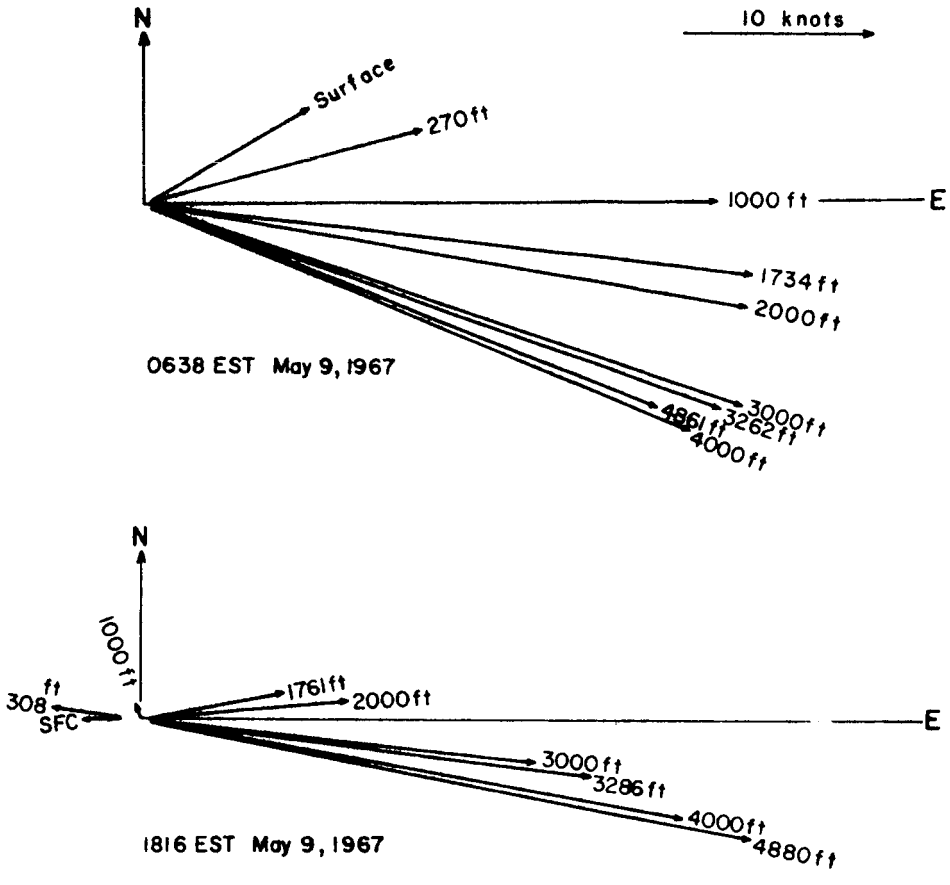

Fig. 29 Wind variation within the Ekman layer.

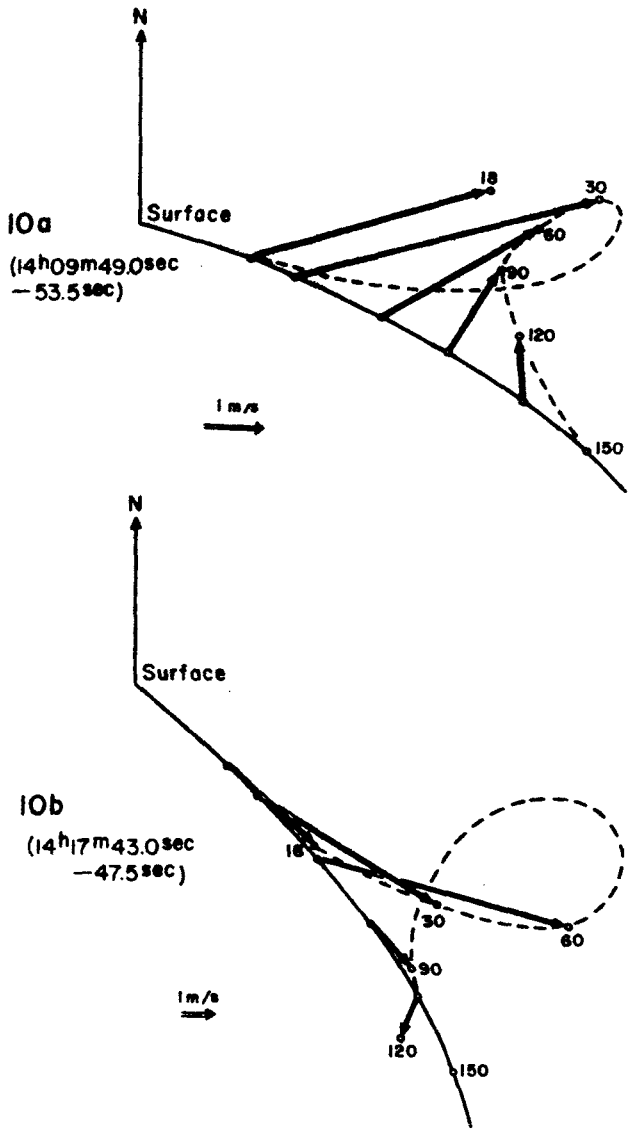

Fig.30 Wind hodograph in the Ekman layer before passage of the cold front (a) and behind the cold front (b). Small numbers indicate height above ground in meters. Arrows show the deviation from the theoretical velocity (solid lines) provided the 150 meter level is on the profile of the Ekman spiral. The dotted lines show hodograph of the actual wind.

this boundary layer is regarded as almost in a barotropic condition. However, assuming that the velocity at the 150 meter level is on the theoretical Ekman spiral distribution, it is clear that the actual wind deviates considerably from the Ekman spiral (Fig. 30), and when hodographs of the actual winds are drawn subjectively in a looplike pattern (18 m in (a) and 120 m in (b) are disregarded), this pattern is too complicated to be solved by using the Ekman-Taylor equation.

4. References

Dennis, W. C., 1965: Analysis of wind tunnel data for several Beckman and Whitley series 50 and Climet model C1-14 anemometers. NASA TMX-53271.

Faller, A. J., 1965: Large eddies in the atmospheric boundary layer and their possible role in the formation of cloud rows. J. Atmos. Sci., 22, 176-184.

Hicks, J. J., and J. K. Angell, 1968: Radar observations of breaking gravitational waves in the visually clear atmosphere. J. Appl. Meteor., 7, 114-121.

Ushijima, T., 1959: Medium-scale waves in the atmosphere. J. M. Soc. Japan, 37, 96-103.

8. CONCLUSIONS

The model airflow of adverse wind conditions at the launch site has been formulated and programmed for use in NASA's computers. Consideration of the effects of friction on the wind nearest the ground have been made and are now being applied to the model. This consideration is unique in its application to thunderstorm outflow winds.

Analysis of NASA meteorological tower data has resulted in several case studies of outflow that contain general wind and temperature characteristics not known before. The sequence of wind and temperature change prior to and during the passage of a storm has been established, with the added bonus of the discovery that a harbinger may exist to help forecast the adverse conditions. The change in wind direction prior to increase in speed can be used to trip a mechanical safety device to stabilize the vehicle during exposure to these winds. The recording of 5 second period oscillation, associated in one case with a flank of the moving cold air, may be useful for warning during marginal situations when a storm is passing nearby. The information that these oscillations extend into warm air can be used in warning systems in the future, when there will be a greater necessity for launchings during inclement weather. The periods between wind speed maximums in cold air indicate that the outflow air spreads in surges. These surges at prescribed time intervals

may be the result of frictional interaction with the ground, or they may be due to oscillatory changes in the precipitation-evaporation mechanism which generates the outflow.

The modification of the theoretical outflow model with data from case studies is hampered by our lack of data containing time variations of the two dimensional horizontal distribution; since the available data from the WIND network for that capability have a resolution of 30 minutes. Five minute averages would enhance our efforts, while one minute resolution would make the network data perfectly integrated with the NASA tower data. But without this horizontal capability the modification process must continue slowly, until a sufficient number of cases have occurred to distribute tower data throughout the storm.[1]

Of the outflow cases studied in detail with tower data, none have shown any disagreement with the basic philosophy of the theoretical model, which states that the cold air moves through the environmental air in the manner of classical hydrodynamic barrier flow. The sequence of wind direction change prior to speed increase coincides with the difluence in streamlines prior to encountering the boundary streamline that forms the

[1] However the restrictions which necessitate combining data from different storms to make up an empirical model is one with which most mesometeorologists have learned to contend. This has been the case also with hurricane researchers and other storm researchers, who are forced by lack of laboratory control to use the case study approach.

leading edge of the moving barrier.

During this year of concentrated effort toward formulating the dynamic forecasting model for adverse wind conditions we have made definite contributions to the state of the art. These contributions include a working digital computer program (the only one of its kind) that models three-dimensional thunderstorm outflow, which that can be modified simply by adding subprograms to compute details as they become available from theory and measurement in the future. In addition to describing the sequence of wind and temperature change associated with thunderstorm outflow, a significant contribution may result from treating the boundary layer flow as a real-time forecasting problem.

9. FUTURE WORK

With the above contributions to thunderstorm research, we now concentrate on obtaining input parameters for the forecasting model. These parameters include the storm location and its motion and intensity, to be derived from radar observations, and the visual data newly acquired from time-lapse photographs of the clouds. The photographs will be an additional asset to the research effort since now the onset of precipitation (resulting in the onset of outflow) can be measured visually and correlated with the size and intensity of the radar echo. The use of autographic records from nearby weather stations will help bridge the gap between the large scale forecast of convective instability, made for Florida in the morning hours, and our individual thunderstorm forecast of high winds at the launch site. Additional radiosonde stations in Florida would provide needed detail in the stability forecast as well as more detailed upper air flow for our local forecasts of storm motion. More case studies containing more high resolution data are being completed and new cases of outflow measured at KSC are forthcoming from NASA, complete with measured network wind and temperature, radar echoes, and time-lapse photographs. When these data are incorporated into this project the modification of the outflow model and the testing with inputs will be completed.

ACKNOWLEDGMENTS

The authors wish to acknowledge the able efforts of the administrative and clerical support of the personnel of the Institute for Storm Research, supervised by Robert Stacy and Jeanette Cockrell.

Particular mention is made of the assistance of Josephine Parrish, who edited the report, and Rebecca Fletcher, who helped organize, guide and supervise its completion. The authors are indeed grateful for their patience and support.

Much of the technical work was discussed with George Fichtl, John Kaufman and Kelly Hill of NASA, who were of considerable help in coordinating our efforts.

Our special thanks go to William W. Vaughn for his critical review and constructive recommendations for this report.

REFERENCES

Atlas, David, et al., 1963: Severe local storms. Meteorol. Monogr., 5, 27, Amer. Meteorol. Soc., Boston, Mass., 247 pp.

Brook, R. R., and K. T. Spillane, 1968: The effect of averaging time and sample duration or estimation and measurement of maximum wind gusts. J. Appl. Meteorol., 7, 4, 567-574.

Brooks, Edward M., 1963: Discussions of Ludlam's paper. Meteorol. Monogr., 5, 27, p. 31.

Browning, Keith A., and Tetsuya Fujita, 1965: A family outbreak of severe local storms--a comprehensive study of the storms in Oklahoma on 26 May 1963. AFCRL-65-695(1), 54 pp.

Byers, H. R., and R. R. Braham, 1949: The thunderstorm. Washington, D.C., U. S. Goverment Printing Office, 287 pp.

Charba, J. and Y. Sasaski, 1967: Relations between the structure and movement of severe storms as revealed from mesonetwork data. Proc., 5th Conf. on Severe Local Storms, St. Louis, 238-245.

Dabbert, Walter F., 1968: Tower induced errors in wind profile measurements. J. Appl. Meteorol., 7, 3, 359-366.

Darkow, Grant L., 1968: The total energy environment of severe storms. J. Appl. Meteorol., 7, 2, 199-205.

_____, 1969: Deflecting forces of non-rotation convective systems due to environmental shear. To be presented at the Amer. Meteorol. Soc. Meeting in April, 1969.

Davis, Francis K., and Herman Newstein, 1968: The variation of gust factors with mean wind speed and with height. J. Appl. Meteorol., 7, 3, 322-328.

Dennis, W. C., 1965: Analysis of wind tunnel data for several Beckman and Whitley series 50 and Climet model C1-14 anemometers. NASA TMX-53271.

Dyer, A. J., 1968: An evaluation of eddy flux variation in the atmospheric boundary layer. J. Appl. Meteorol., 7, 5, 845-850.

Faller, A. J., 1965: Large eddies in the atmospheric boundary layer and their possible role in the formation of cloud rows. J. Atmos. Sci., 22, 176-184.

Fichtl, George H., 1968: An analysis of the roughness length associated with the NASA 150-meter meteorological tower. NASA TMX-53690.

_____, 1968: Characteristics of turbulence observed at the NASA 150-m meteorological tower. J. Appl. Meteorol., 7, 5, 838-844.

Fujita, Tetsuya, 1962: A review of researches on analytical mesometeorology. Mesometeorology Project Research Paper No. 8, Department of Geophysical Sciences, University of Chicago, 114 pp.

_____, 1963: Analytical mesometeorology: a review. Meteorol. Monogr., 5, 77-128.

Gerrish, H. P., and H. W. Hiser, 1965: Mesoscale studies of instability patterns and winds in the tropics. Rept. No. 8, Institute of Marine Science, University of Miami.

Goldman, J. L., 1967: A parameterized model of air circulation and rain distribution in severe storms. Final Rept., NSSL, Contract No. E-36-67(N), ISR, Houston, 76 pp.

_____, 1968: The high speed updraft--the key to the severe thunderstorm. J. Atmos. Sci., 25, 2, 222-248.

_____, and J. C. Freeman, 1966: The development of a model of air circulation and rain distribution in a steady state severe storm. Final Rept., NSSL, Contract No. Cwb-11367, ISR, Houston, 55 pp.

_____, and P. W. Sloss, 1969: Structure of the leading edge of thunderstorm cold air outflow. Submitted to 6th Conference on Severe Local Storms, Chicago, April 8-10, 1969.

Hicks, J. J., and J. K. Angell, 1968: Radar observations of breaking gravitational waves in the visually clear atmosphere. J. Appl. Meteorol., 7, 114-121.

Kaufman, J. W., and L. F. Keene, 1968: NASA's 150-meter meteorological tower located at the Kennedy Space Center, Florida. NASA TMX-53699.

Ligda, M. G. H., and S. G. Bigler, 1958: Radar echoes from a cloudless cold front. J. Meteorol., 15, 494-501.

Lumley, J. T., and H. A. Panofsky, 1964: The Structure of Atmospheric Turbulence. New York, Interscience Publishers, John Wiley and Sons, Inc.

Milne-Thomson, L. M., 1950: Theoretical hydrodynamics. New York, The Macmillan Co., 632 pp.

Orville, Harold D., 1967: Ambient wind effects on the initiation and development of cumulus clouds over mountains--a numerical experiment. Presented at the Nat'l. Amer. Meteorol. Soc. Meeting, New York, January 23-26.

Panofsky, H. A., et al., 1958: The relation between Eulerian time and space spectra. Quart. J. Roy. Meteorol. Soc., 84, 270.

Peskov, B. Ye, and A. I. Snitkovskiy, 1968: Forecasting heavy squalls. Meteorologiya i gidrologiya, 9, 52-57.

Rider, N. E., 1954: Eddy diffusion of momentum, water vapor and heat near the ground. Phil. Trans. Roy. Soc., A246, 481.

Sasaki, Yoshikazu and Sigekata Syono, 1966: Motion of the vortex with pressure and inflow which are not circular symmetry. No. ARL-1470-3, U. of Okla. Research Institute, Atmospheric Research Laboratory, Norman, Oklahoma.

Ushijima, T., 1959: Medium-scale waves in the atmosphere. J. M. Soc. Japan, 37, 96-103.

Weinstein, A. I., and L. G. Davis, 1968: A parameterized numerical model of cumulus convection. Rept. No. 11, Contract GA-777, National Science Foundation, Department of Meteorology, Pennsylvania State University, University Park, 44pp.